immunodeficiency virus reverse transcriptase using an alpha-boranophosphate nucleoside analogue. J Biol Chem 2001;276(51):48466–72.
Shirasaka T, Kavlick MF, Ueno T, Gao WY, Kojima E, Alcaide ML, et al. Emergence of human immunodeficiency virus type 1 variants with resistance to multiple dideoxynucleosides in patients receiving therapy with dideoxynucleosides. Proc Natl Acad Sci USA 1995;92(6):2398–402.
Srinivas RV, Fridland A. Antiviral activities of 9-*R*-2-phosphonomethoxypropyl adenine (PMPA) and bis(isopropyloxymethylcarbonyl)PMPA against various drug-resistant human immunodeficiency virus strains. Antimicrob Agents Chemother 1998;42(6):1484–7.
Starnes MC, Cheng YC. Cellular metabolism of 2′,3′-dideoxycytidine, a compound active against human immunodeficiency virus in vitro. J Biol Chem 1987;262(3):988–91.
Tuske S, Sarafianos SG, Clark Jr AD, Ding J, Naeger LK, White KL, et al. Structures of HIV-1 RT-DNA complexes before and after incorporation of the anti-AIDS drug tenofovir. Nat Struct Mol Biol 2004;11(5):469–74.
Wainberg MA, Drosopoulos WC, Salomon H, Hsu M, Borkow G, Parniak M, et al. Enhanced fidelity of 3TC-selected mutant HIV-1 reverse transcriptase. Science 1996;271(5253):1282–5.
Weiner MP, Costa GL, Schoettlin W, Cline J, Mathur E, Bauer JC. Site-directed mutagenesis of double-stranded DNA by the polymerase chain reaction. Gene 1994;151(1–2):119–23.
Winters MA, Coolley KL, Girard YA, Levee DJ, Hamdan H, Shafer RW, et al. A 6-basepair insert in the reverse transcriptase gene of human immunodeficiency virus type 1 confers resistance to multiple nucleoside inhibitors. J Clin Invest 1998;102(10):1769–75.
Yoshimura K, Feldman R, Kodama E, Kavlick MF, Qiu YL, Zemlicka J, et al. In vitro induction of human immunodeficiency virus type 1 variants resistant to phosphoralaninate prodrugs of *Z*-methylenecyclopropane nucleoside analogues. Antimicrob Agents Chemother 1999;43(10):2479–83.

ANTIMICROBIAL AGENTS AND CHEMOTHERAPY, June 2008, p. 2111–2119 Vol. 52, No. 6
0066-4804/08/$08.00+0 doi:10.1128/AAC.01299-07

Potent Synergistic Anti-Human Immunodeficiency Virus (HIV) Effects Using Combinations of the CCR5 Inhibitor Aplaviroc with Other Anti-HIV Drugs[▽]

Hirotomo Nakata,[1,2] Seth M. Steinberg,[3] Yasuhiro Koh,[2] Kenji Maeda,[1] Yoshikazu Takaoka,[4] Hirokazu Tamamura,[5] Nobutaka Fujii,[5] and Hiroaki Mitsuya[1,2]*

Experimental Retrovirology Section, HIV and AIDS Malignancy Branch, Center for Cancer Research, National Cancer Institute, National Institutes of Health, Bethesda, Maryland 20892[1]; Kumamoto University Graduate School of Medical and Pharmaceutical Sciences, Departments of Infectious Diseases and Hematology, Kumamoto 860-8556, Japan[2]; Biostatistics and Data Management Section, Center for Cancer Research, National Cancer Institute, National Institutes of Health, Bethesda, Maryland 20892[3]; Ono Pharmaceutical Co. Ltd., Osaka 618-8585, Japan[4]; and Graduate School of Pharmaceutical Sciences, Kyoto University, Sakyo-ku, Kyoto 606-8501, Japan[5]

Received 8 October 2007/Returned for modification 19 November 2007/Accepted 21 March 2008

Aplaviroc (AVC), an experimental CCR5 inhibitor, potently blocks in vitro the infection of R5-tropic human immunodeficiency virus type 1 (R5-HIV-1) at subnanomolar 50% inhibitory concentrations. Although maraviroc is presently clinically available, further studies are required to determine the role of CCR5 inhibitors in combinations with other drugs. Here we determined anti-HIV-1 activity using combinations of AVC with various anti-HIV-1 agents, including four U.S. Food and Drug Administration-approved drugs, two CCR5 inhibitors (TAK779 and SCH-C) and two CXCR4 inhibitors (AMD3100 and TE14011). Combination effects were defined as synergistic or antagonistic when the activity of drug A combined with B was statistically greater or less, respectively, than the additive effects of drugs A and A combined and drugs B and B combined by using the Combo method, described in this paper, which provides (i) a flexible choice of interaction models and (ii) the use of nonparametric statistical methods. Synergistic effects against R5-HIV-$1_{Ba\text{-}L}$ and a 50:50 mixture of R5-HIV-$1_{Ba\text{-}L}$ and X4-HIV-$1_{ERS104pre}$ (HIV-$1_{Ba\text{-}L/104pre}$) were seen when AVC was combined with zidovudine, nevirapine, indinavir, or enfuvirtide. Mild synergism and additivity were observed when AVC was combined with TAK779 and SCH-C, respectively. We also observed more potent synergism against HIV-$1_{Ba\text{-}L/104pre}$ when AVC was combined with AMD3100 or TE14011. The data demonstrate a tendency toward greater synergism with AVC plus either of the two CXCR4 inhibitors compared to the synergism obtained with combinations of AVC and other drugs, suggesting that the development of effective CXCR4 inhibitors may be important for increasing the efficacies of CCR5 inhibitors.

CCR5 is a member of the G-protein-coupled, seven-transmembrane-segment receptors, which comprise the largest superfamily of proteins in the body (30). In 1996, it was revealed that CCR5 serves as one of the two essential coreceptors for the entry of human immunodeficiency virus type 1 (HIV-1) into human $CD4^+$ cells, thereby serving as an attractive target for possible interventions against HIV-1 infection (1, 9, 40, 42). Consequently, scores of small-molecule CCR5 inhibitors which exert potent activity against R5-tropic HIV-1 (R5-HIV-1) were identified (2, 10, 19, 35). Aplaviroc (AVC), a spirodiketopiperazine derivative, represents one such experimental small-molecule CCR5 inhibitor (17, 18). AVC binds to human CCR5 with a high affinity, blocks HIV-1 gp120 binding to CCR5, and exerts potent activity against a wide spectrum of laboratory and primary R5-HIV-1 isolates, including multidrug-resistant HIV-1 isolates (50% inhibitory concentrations, 0.2 to 0.6 nM) (17, 18). Maraviroc (MVC) is another small-molecule CCR5 inhibitor which has become the first CCR5 inhibitor approved for the treatment of AIDS and HIV-1 infection by the U.S. Food and Drug Administration (FDA). One possible concern over the long-term use of CCR5 inhibitors is the change of viral tropism, which enables the virus to use the CXCR4 receptor (20, 41); therefore, CCR5 inhibitors are unlikely to be used as single agents. Assessments of the interaction of CCR5 inhibitors with other anti-HIV-1 agents should thus help provide an understanding of the role of CCR5 inhibitors and help design regimens to be used for the treatment of individuals infected with HIV-1.

In the present study, we determined the effects against R5-HIV-$1_{Ba\text{-}L}$ of AVC in combination with various anti-HIV-1 agents which affect other steps of the viral life cycle, including a nucleoside reverse transcriptase inhibitor, zidovudine (ZDV); a nonnucleoside reverse transcriptase inhibitor, nevirapine (NVP); a protease inhibitor, indinavir (IDV); and a fusion inhibitor, enfuvirtide (ENF). We assessed the synergistic effects of AVC in combination with CXCR4 inhibitors as well as the other drugs described above against a mixture of R5-HIV-$1_{Ba\text{-}L}$ and X4-HIV-$1_{ERS104pre}$ (designated HIV-$1_{Ba\text{-}L/104pre}$). In the present study, we also developed an evaluation system, designated the Combo method, which provides (i) a flexible choice of interaction models, (ii) the use of nonparametric statistical methods to obtain *P* values for comparison, and (iii) flexibility with respect to experimental design (e.g., checkerboard and constant-ratio designs). The present data suggest that AVC exerts antiviral synergy when it is

* Corresponding author. Mailing address: Departments of Infectious Diseases and Hematology, Kumamoto University School of Medicine, 1-1-1 Honjo, Kumamoto 860-8556, Japan. Phone: (81) 96-373-5156. Fax: (81) 96-363-5265. E-mail: hm21q@nih.gov.

▽ Published ahead of print on 31 March 2008.

used with other classes of anti-HIV-1 agents but apparently not when it is used with other CCR5 inhibitors. The present data also demonstrate a tendency toward greater synergism with AVC plus either of the two CXCR4 inhibitors examined in comparison to the synergism obtained with combinations of AVC and other FDA-approved drugs, suggesting that the development of effective CXCR4 inhibitors may be important for increasing the efficacies of CCR5 inhibitors.

MATERIALS AND METHODS

Antiviral agents. AVC is an experimental CCR5 inhibitor containing a spirodiketopiperazine core, as described previously (18, 19, 26). TAK779, SCH-C, and AMD3100 were synthesized as described previously (2, 7, 35). ZDV was purchased from Sigma (St. Louis, MO). IDV was kindly provided by Japan Energy Inc. (Tokyo, Japan). TE14011 and ENF were synthesized as described previously (36, 37). NVP was a kind gift from Boehringer Ingelheim Pharmaceuticals Inc. (Ridgefield, CT).

Viruses. R5-HIV-$1_{Ba\text{-}L}$ was obtained from the AIDS Research and Reference Reagent Program (13). X4-HIV-$1_{ERS104pre}$ was isolated from a drug-naïve patient with AIDS (33). These HIV-1 isolates were propagated in phytohemagglutinin-stimulated peripheral blood mononuclear cells (PHA-PBMCs), and the culture supernatants were harvested and stored at −80°C until use (22). In certain experiments, a 50:50 mixture of HIV-$1_{Ba\text{-}L}$ and HIV-$1_{ERS104pre}$ (HIV-$1_{Ba\text{-}L/104pre}$) was prepared.

Assay for in vitro anti-HIV-1 activity. PBMCs were isolated from the buffy coats of HIV-1-seronegative individuals by Ficoll-Hypaque density gradient centrifugation and were cultured at a concentration of 10^6 cells/ml in RPMI 1640-based culture medium supplemented with 10% fetal calf serum (FCS; HyClone Laboratories, Logan, UT), penicillin (50 U/ml), and streptomycin (50 μg/ml) (10% FCS–RPMI) with 10 μg/ml PHA for 3 days prior to the anti-HIV-1 activity assay in vitro. PHA-PBMCs (10^6/ml) from a 3-day culture were resuspended in 10% FCS–RPMI containing 10 ng/ml interleukin-2 and plated into each well of 96-well microculture plates (10^5 per well). Each of the test compounds was added as a single agent or in combination with another agent to each well of the microculture plates. For assessment of the effects of a combination of any two drugs, three threefold serial concentrations were chosen on the basis of the dose-response curve at which the percent inhibition values increased linearly.

The cells were subsequently exposed to 50 50% tissue culture infectious doses ($TCID_{50}$s) of HIV-$1_{Ba\text{-}L}$ or a mixture of 25 $TCID_{50}$s of HIV-$1_{Ba\text{-}L}$ and 25 $TCID_{50}$s of HIV-$1_{ERS104pre}$ and incubated at 37°C in humidified air containing 5% CO_2. On day 7 of culture, the cell-free culture supernatants were harvested and the HIV-1 p24 antigen levels in the supernatants were determined with a fully automated chemiluminescent enzyme immunoassay system (Lumipulse F; Fujirebio Inc., Tokyo, Japan) (18, 23). All the assays were performed in duplicate, and each experiment was conducted on 5 to 10 different occasions. No cytotoxicity was observed at the highest concentrations of each agent, as assessed by the trypan blue dye exclusion method.

Mathematical analysis: the Combo method. We assessed the effects of drug combinations using the combination index (CI), calculated with CalcuSyn software (BioSoft, Cambridge, United Kingdom), which was based on the median-effect method developed by Chou and Talalay (3, 4). For experiments with combinations of the same drug, serially diluted drug concentrations were chosen on the basis of the 50% effective concentrations (EC_{50}s), and each drug was combined with itself at the same concentration. As in the original method, CIs of <1, 1, and >1 were judged to represent synergism, additivity, and antagonism, respectively.

It should be noted that the Chou and Talalay median-effect method (3, 4) alone does not allow us to statistically compare the effects of the combinations. Thus, we devised a new method for evaluation of the effects of drug combinations, designated the Combo method. For the Combo method used in the present study, we used three concentrations of one drug (drug A) and three concentrations of the other drug (drug B) and combined the drugs at three different concentrations, preparing nine (3 × 3) combination cultures, and we obtained nine determinations of HIV-1 p24 concentrations (each combination assay was performed in duplicate). More precisely, three combinations were examined: the same drug A combination (drug A and drug A), the same drug B combination (drug B and drug B), and the combination of drug A and drug B. A full view of the data obtained with the drug combinations can be visualized (as shown in the Results section) in three-dimensional (3-D) figures by the use of Microsoft Excel software (version 11.0, 2004; Microsoft Corporation, Redmond, WA), based on the method of Prichard and colleagues (27, 28, 29). It is of note that with the Bliss independence method, the predicted additive effects at each combination point are subtracted from the inhibitory effects of the combination determined from the experimental drug combination assay, generating percent synergy values, and the points plotted above the predicted additive effects represent synergism, while the points below the plane represent antagonism. Using the Bliss independence method, we calculated percent synergy values for the nine determinations described above, and the average value was further computed, generating a mean percent synergy value (%$synergy^{mean}$). We repeated this assay for each drug combination 5 or 10 times on different occasions. These 5 or 10 %$synergy^{mean}$ values thus obtained for a set of combinations (drug A-drug A, drug B-drug B, and drug A-drug B) were compared with the other data sets (5 or 10 %$synergy^{mean}$ values) by the Wilcoxon rank sum test, generating P values for each combination set. All P values are two-tailed and have not been formally adjusted for multiple comparisons. However, in the context of the several experiments and comparisons performed, P values of <0.01 would clearly indicate statistical significance, while differences with values of $0.01 < P < 0.05$ would indicate strong trends.

TABLE 1. Anti-HIV-1 activity of each drug in the assay system

Virus	Compound	EC (nM) for anti-HIV-1 activity[a]			
		50%	75%	90%	95%
Ba-L	AVC	0.7 ± 0.4	4.0 ± 4.0	16 ± 15	25 ± 14
	SCH-C	6.8 ± 6.0	31 ± 18	94 ± 43	131 ± 64
	TAK779	20 ± 14	127 ± 83	332 ± 192	576 ± 224
	ZDV	18 ± 4.0	58 ± 3.0	128 ± 54	178 ± 49
	NVP	19 ± 2.0	36 ± 11	127 ± 39	149 ± 47
	IDV	29 ± 7.0	44 ± 12	75 ± 18	87 ± 13
	ENF	11 ± 4.0	46 ± 5.0	82 ± 14	98 ± 16
104pre	AMD3100	26 ± 8.0	96 ± 21	193 ± 51	257 ± 46
	TE14011	4.0 ± 1.0	16 ± 7.0	50 ± 11	78 ± 17

[a] The EC_{50}, EC_{75}, EC_{90}, and EC_{95} values were determined by using PHA-PBMCs isolated from three different donors and the inhibition of p24 Gag protein production as the end point. All assays were conducted in triplicate. The results shown represent the arithmetic means (±1 standard deviation) of the values from three independently conducted assays.

RESULTS

Activities of anti-HIV-1 agents in PHA-PBMCs. We first determined the antiviral potencies of seven anti-HIV-1 agents (AVC, SCH-C, TAK779, ZDV, NVP, IDV, and ENF) against HIV-$1_{Ba\text{-}L}$ employing PHA-PBMCs as target cells (Table 1). AVC had a potent inhibitory effect against HIV-$1_{Ba\text{-}L}$, with mean EC_{50}, EC_{75}, EC_{90}, and EC_{95} values of 0.7, 4, 16, and 25 nM, respectively. SCH-C and TAK779, which are both CCR5 inhibitors, also showed potent antiviral activity (but with less potent antiviral activity compared to that of AVC), with EC_{50}s of 6 and 20 nM, respectively. To determine the additive effects of AVC-AVC and AMD3100-AMD3100, we employed R5-HIV-$1_{Ba\text{-}L}$ and X4-HIV-$1_{ERS104pre}$ as the virus inocula, respectively, since AVC is inert against X4-HIV-1 and AMD3100 is inert against R5-HIV-1. These two agents were found to be potent against the virus, with EC_{50}s of 26 and 4 nM, respectively. No toxicity of any of the anti-HIV-1 agents was observed at concentrations up to 1.0 μM, as determined by examination of PHA-PBMCs (data not shown).

Same-drug combination and additivity. To determine whether combinations of two different anti-HIV-1 agents produced synergistic, additive, or antagonistic effects, we first attempted to establish an algorithm so that the effects of the combination of the same drug (i.e., drug A-drug A) represent

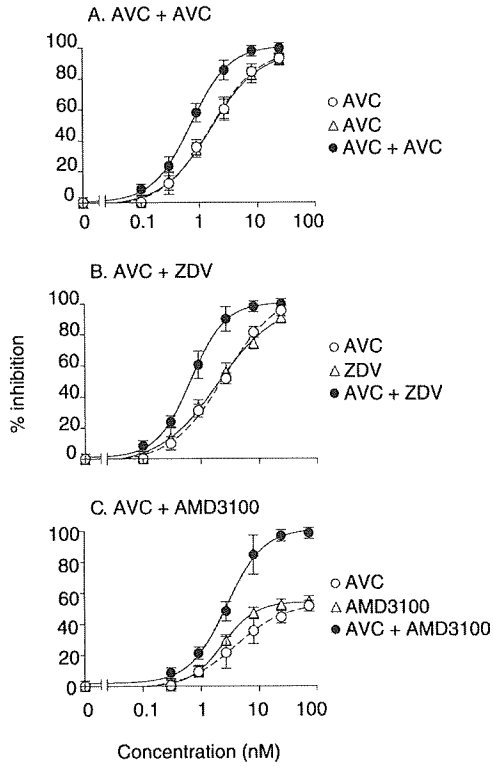

FIG. 1. Dose-response curves of single and combined drug assays. Three representative dose-response curves are shown. (A) Dose-response curve with the same-drug combination (AVC-AVC). PHA-PBMCs were exposed to R5-HIV-1_{Ba-L} and cultured in the presence of AVC alone or AVC-AVC over 7 days. AVC was serially diluted threefold to give concentrations in the range of 0.1 to 24.3 nM. The percent inhibition values were determined on the basis of the amounts of p24 Gag proteins in the culture supernatants. (B) AVC was combined with ZDV at a fixed ratio (1:11), and the assay was conducted as described above for panel A. (C) AVC (concentration range, 0.3 to 72.9 nM) was combined with AMD3100 at a 1:11 ratio. PHA-PBMCs were exposed to a 50:50 mixture of R5-HIV_{Ba-L} and X4-HIV-$1_{ERS104pre}$ and cultured in the presence of AVC alone, AMD3100 alone, or AVC-AMD3100. All assays were performed on 5 to 10 different occasions, and all the values shown represent the arithmetic means ± 1 standard deviation.

additivity. We determined the effects of combinations of the same drug for each of the seven anti-HIV-1 agents using the CIs dictated by the median-effect method (4). Figure 1A shows three representative dose-response curves of the percent inhibition of HIV-1 replication in the presence of a CCR5 inhibitor (AVC) alone, a reverse transcriptase inhibitor (ZDV) alone, a CXCR4 inhibitor (AMD3100) alone, or AVC plus AVC, ZDV, or AMD3100. A range of concentrations at which the percent inhibition values linearly increased was identified (Fig. 1A and B) and was used to examine the effects of any combination of two drugs chosen.

We found that the same-drug combination of AVC-AVC which gave a 50% reduction of HIV-1 replication produced a CI of 1.03 ± 0.09 (Table 2), indicating that this combination produced additivity on the basis of the median-effect method. However, that same-drug combination which gave 75, 90, and 95% reductions in viral replication produced CIs of 0.82, 0.71, and 0.68, respectively, which indicated that this same-drug combination produced synergistic effects. Synergistic effects were similarly indicated when the other anti-HIV-1 agents were examined as same-drug combinations in our analysis (Table 2).

The indication of synergism in the same-drug combination described above was thought to be a limitation or error inherent to the median-effect method or to stem from the variability of the biological data obtained. Since the median-effect method does not provide room for statistical analysis or a full view of the combination data, we examined the same data set using Microsoft Excel software, based on the method of Prichard and colleagues (27, 28, 29), which gives a graphical 3-D view of the entire data set. In the analysis of the AVC-AVC combination data, this method with Microsoft Excel software indicated that the combination of the highest AVC concentration (2.7 nM AVC and 2.7 nM AVC) that produced synergism gave a percent synergy value of 2.2, although other combinations were determined to be additive or antagonistic, giving an average (± standard deviation) percent synergy value of −1.8 ± 2.4 (Fig. 2A). The same-drug combinations of ZDV, NVP, and ENF similarly gave partial synergism (Fig. 2B, C, and E). However, the same-drug combination of IDV indicated synergism with all data points, with an average percent synergy value of 3.6 ± 2.2 (Fig. 2D). We predicted that the partial synergism seen with AVC, ZDV, NVP, and ENF and the entire synergism seen with IDV also represented a limitation or error inherent to the method of Prichard and colleagues (27, 28, 29) or the variability of the biological data obtained.

AVC acts in synergy with ZDV, NVP, IDV, and ENF to block the replication of HIV-1_{Ba-L} in PHA-PBMCs. Considering that one of the main reasons for the partial synergism described above could stem from the variability of the cell-based assay data used in the present work, we used standard nonparametric statistical analysis methods to evaluate the differences. To this end, we conducted the drug-combination assay in duplicate and determined the %$synergy^{mean}$ values in three settings: (i) drug A-drug A, (ii) drug B-drug B, and (iii) drug A-drug B. Experiments testing the drug A-drug A combination and the drug B-drug B combination were conducted on 10 different occasions, while the drug A-drug B combinations assay was conducted on 5 different occasions. As shown in Fig. 3A, as

TABLE 2. CIs against HIV-1 obtained with mixtures of the same compounds at various inhibitory concentrations

Virus	Combination[b]	CI[a]			
		50%	75%	90%	95%
Ba-L	AVC + AVC	1.03 ± 0.09	0.82 ± 0.10	0.71 ± 0.10	0.68 ± 0.09
	ZDV + ZDV	1.08 ± 0.14	0.95 ± 0.18	0.84 ± 0.23	0.81 ± 0.22
	NVP + NVP	0.99 ± 0.09	0.81 ± 0.11	0.69 ± 0.12	0.66 ± 0.14
	IDV + IDV	1.02 ± 0.06	0.91 ± 0.05	0.79 ± 0.07	0.76 ± 0.06
	ENF + ENF	1.04 ± 0.08	0.89 ± 0.08	0.75 ± 0.09	0.73 ± 0.11
104pre	AMD + AMD	1.12 ± 0.12	0.88 ± 0.09	0.69 ± 0.09	0.67 ± 0.10
	TE + TE	1.05 ± 0.15	0.90 ± 0.11	0.80 ± 0.13	0.78 ± 0.13

[a] Drug interactions of same-drug combinations were analyzed by using CIs. CIs were calculated on the basis of the model of Chou and Talalay (3, 4) with CalcuSyn software (BioSoft). Originally, CIs of <1, 1, or >1 indicated a synergistic effect, an additive effect, and antagonism, respectively. The drugs were combined at a 1:1 ratio, and all assays were conducted in duplicate. The results shown represent the arithmetic means (±1 standard deviation) of the CIs at various inhibitory concentrations (50%, 75%, 90%, and 95%) from 10 independently conducted assays.

[b] AMD, AMD3100; TE, TE14011.

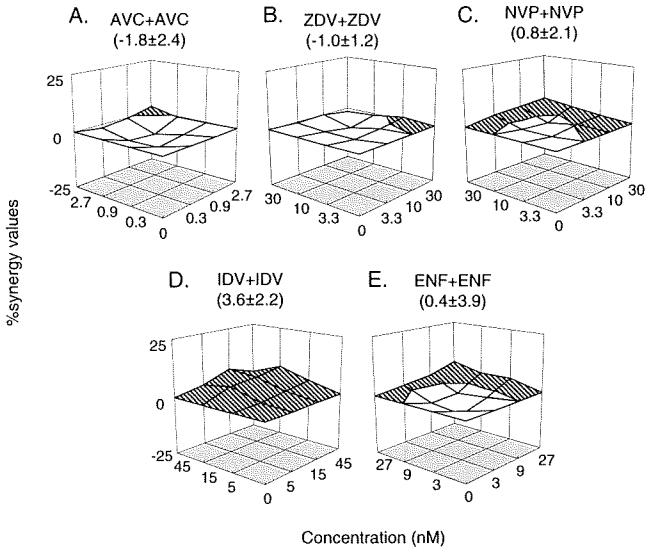

FIG. 2. Effects of same-drug combinations. The serially diluted anti-HIV-1 agents AVC (A), ZDV (B), NVP (C), IDV (D), and ENF (E) were combined with the same agent diluted under the same conditions; PHA-PBMCs were exposed to R5-HIV-1_{Ba-L} and cultured in the presence of the drugs combined. The combination effects (percent synergy values on the vertical z axis) were determined on the basis of the Bliss independence method. In the 3-D graphs, obtained on the basis of the method of Prichard et al. (27, 28, 29), the average percent synergy values at each concentration derived from 10 experiments were plotted. The hatched area represents synergism (percent synergy values, >0), while the open area represents additivity or antagonism (percent synergy values, ≤0). Numbers in parentheses represent the average percent synergy values (±1 standard deviation). The x and y axes indicate the concentrations of the drug tested (nM). All assays were performed in duplicate, and each experiment was independently conducted 10 times.

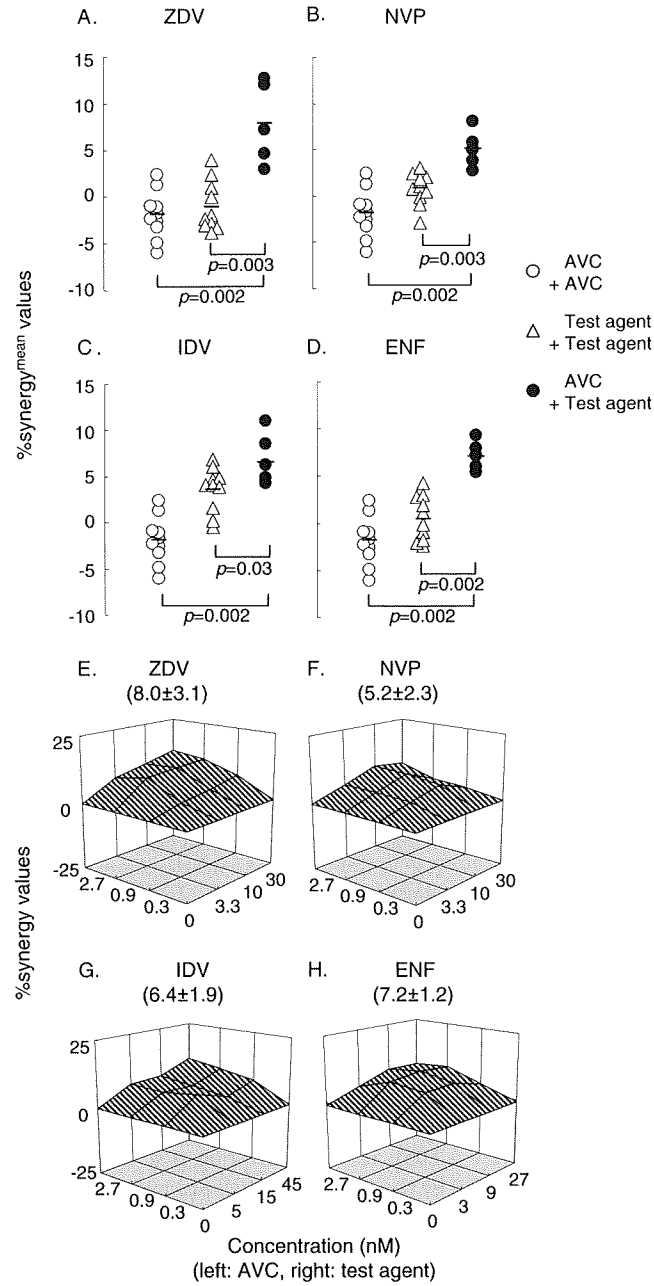

FIG. 3. Effects of AVC in combination with other anti-HIV-1 agents against R5-HIV-1_{Ba-L}. Drug combination assays were conducted, and the %synergy^{mean} values (the mean of the nine percent synergy values from each set of the data) are shown in three settings: (i) AVC-AVC, (ii) test agent (to be combined with AVC)-test agent, and (iii) AVC-test agent (A to D). The AVC-AVC combination and the test agent-test agent combination were tested on 10 different occasions, while the AVC-test agent combination assay was done on 5 different occasions. The differences in the %synergy^{mean} values between the three settings were analyzed by using the Wilcoxon rank sum test. The short bars indicate the arithmetic means. The combination effects are also shown in 3-D graphs, as determined on the basis of the method of Prichard et al. (see the legend to Fig. 2).

expected, the same-drug combination assays with AVC and ZDV produced relatively low average %synergy^{mean} values of −1.8 and −1.0, respectively. However, the AVC-ZDV combination gave a high average %synergy^{mean} value of 8.0. When we examined the difference among the AVC-AVC, ZDV-ZDV, and AVC-ZDV data using the Wilcoxon rank sum test, there was a statistically significant difference between the AVC-AVC and the AVC-ZDV data (P = 0.002) as well as between the ZDV-ZDV and the AVC-ZDV data (P = 0.003). The same was true when we examined the effects of NVP, IDV, and ENF in combination with AVC (Fig. 3B to D). With these data, we determined that if both the drug A-drug A and drug B-drug B combinations gave relatively low %synergy^{mean} values and a significant difference between the drug A-drug B combination and the same-drug combinations was detected, we would judge that there was significant synergism. When we plotted the average percent synergy value for the combination of drugs A and B at each different concentration on a point-by-point basis by the method of Prichard and colleagues (27, 28, 29), the results showed substantially higher levels of synergism for all data points (Fig. 3E to H). The average percent synergy values for AVC-ZDV, AVC-NVP, AVC-IDV, and AVC-ENF were 8.0 ± 3.1, 5.2 ± 2.3, 6.4 ± 1.9, and 7.2 ± 1.2, respectively, which corroborated the interpretation of the data shown in Fig. 3A to D. Thus, we interpreted that the addition of AVC to each of the other agents produced significant synergism.

Effects of AVC in combination with SCH-C or TAK779 against R5-HIV-1_{Ba-L}. We next asked whether AVC in combi-

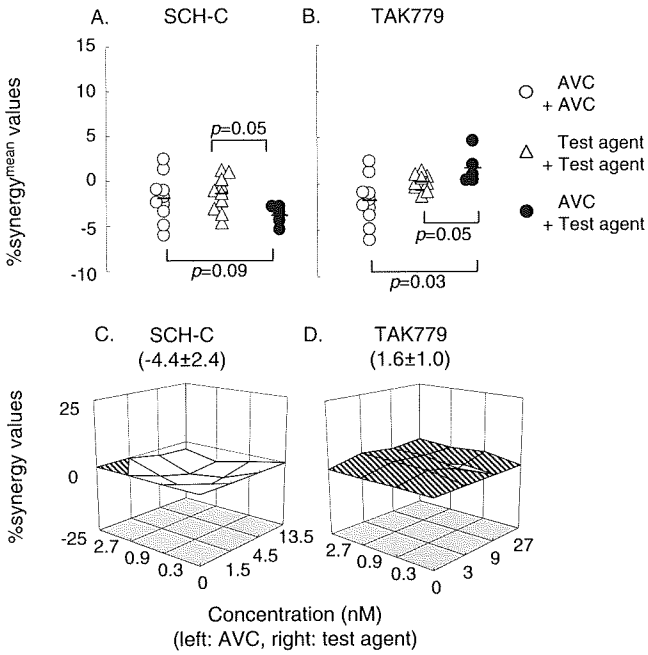

FIG. 4. Effects of AVC in combination with other CCR5 inhibitors. The effects of AVC in combination with SCH-C (A) or TAK779 (B) when they were exposed to R5-HIV-1_{Ba-L} are shown. No significant synergism was seen when AVC was combined with SCH-C or TAK779 compared with that seen with AVC-AVC. There was a trend toward antagonism when AVC–SCH-C with SCH-C–SCH-C and a trend toward synergism when AVC-TAK779 was compared with TAK779-TAK779. When these data were examined by the method of Prichard et al. (27, 29), AVC–SCH-C showed a mixed pattern but with an inclination toward antagonism (C), while AVC-TAK779 showed a mixed pattern but with an inclination toward synergy (D).

nation with SCH-C or TAK779 had synergistic activity against HIV-1_{Ba-L} (Fig. 4). The difference between the AVC-AVC and the AVC–SCH-C combinations was not statistically significant ($P = 0.09$), while there was evidence of a trend toward antagonism between the SCH-C–SCH-C and the AVC–SCH-C combinations ($P = 0.05$). It was interesting that when these data were examined by the method of Prichard and colleagues (27, 28, 29), a mixed pattern with an inclination toward antagonism was seen, with an average percent synergy of -4.4 ± 2.4. We also examined whether AVC had significant combination effects when it was combined with TAK779. There was a trend toward a statistically significant difference between AVC-AVC and AVC-TAK779 ($P = 0.03$) as well as TAK779-TAK779 and AVC-TAK779 ($P = 0.05$). However, when these data were plotted in the chart by the method of Prichard and colleagues (27, 28, 29), the pattern was a mixed one, with a low average percent synergy (1.6 ± 1.0), suggesting that synergism would be at a low level. However, it was noted that the same set of data for the combination of AVC and SCH-C produced CI values of 1.05 (at a 50% inhibitory effect) and 0.58 (at a 90% inhibitory effect), indicating that there was synergism between AVC and SCH-C, as analyzed on the basis of the median-effect method of Chou and Talalay (3, 4). It was thought that there was a propensity toward an overestimation of the combination effects toward synergism when the median-effect method was used.

Combination effects of AVC in a mixture of R5-HIV-1_{Ba-L} and X4-HIV-$1_{ERS104pre}$. AVC exerts no antiviral activity against X4-HIV-1 (18, 23), although the HIV-1 population seen in individuals with HIV-1 infection often comprises both R5- and X4-HIV-1 populations. Hence, it would be reasonable to use a CCR5 inhibitor plus a CXCR4 inhibitor to treat individuals with HIV-1 infection (6). Thus, we attempted to examine effects of the combination of AVC and either AMD3100 and TE14011 against HIV-$1_{Ba-L/104pre}$.

It is thought that the replication kinetics of HIV-1 strains tend to affect the results of any antiviral assay, in particular, when more than one HIV-1 isolate is employed in one assay. We therefore first conducted a set of experiments in order to delineate the replication curves for both the R5-tropic (HIV-1_{Ba-L}) and X4-tropic (HIV-$1_{ERS104pre}$) strains used in this study. It was confirmed that the two strains had comparable replication kinetics and that the p24 values of both strains were comparable over 7 days when the amount of each strain inoculated was adjusted on the basis of the $TCID_{50}$ for the strain (data not shown). Moreover, the amounts of HIV-1 p24 produced by PBMCs that were exposed to the mixture of the R5- and X4-tropic strains and cultured in the presence of a high concentration of AVC were comparable to the amounts of HIV-1 p24 from PBMCs that were similarly treated but that were cultured in the presence of a high concentration of AMD3100 (Fig. 1C). These data suggested that HIV-1_{Ba-L} and HIV-$1_{ERS104pre}$ replicate comparably in cell cultures inoculated with the 50:50 mixture of the viruses. To determine the additive effects of AVC-AVC and AMD3100-AMD3100, we employed R5-HIV-1_{Ba-L} and X4-HIV-$1_{ERS104pre}$ as the target viruses, respectively, since AVC is inert against X4-HIV-1 and AMD3100 is inert against R5-HIV-1.

The AVC-AMD3100 combinations produced %synergy^{mean} values significantly different from those for AVC-AVC ($P = 0.002$) and those for AMD3100-AMD3100 ($P = 0.005$) (Fig. 5A). When these combination data were examined in the 3-D model of Prichard and colleagues (27, 28, 29), apparently high levels of synergism were seen for all data points, with an average percent synergy value of 8.0 ± 4.4 (Fig. 5G). When TE14011 was combined with AVC, synergism was similarly seen, with an average percent synergy value of 8.2 ± 4.5 (Fig. 5H). The %synergy^{mean} values for AVC-ENF were also greater than those for AVC-AVC ($P = 0.005$) and less than those for ENF-ENF ($P = 0.04$); however, when the level of synergism was examined in the 3-D model, it appeared to be relatively lower, with an average percent synergy value of 4.8 ± 4.2 (Fig. 5I).

We next examined the effect of AVC in combination with one of the three FDA-approved anti-HIV-1 agents, ZDV, NVP, and IDV. The %synergy^{mean} values obtained with AVC-ZDV or AVC-NVP were greater than those obtained with AVC-AVC, ZDV-ZDV, and NVP-NVP (P values for all comparisons, ≤ 0.005; Fig. 5D and E). In the 3-D model, synergism was also observed for ZDV and NVP in combination with AVC (Fig. 5J and K). AVC-IDV produced no significant difference in the %synergy^{mean} values compared to those for IDV-IDV ($P = 0.2$), although the effect of AVC-IDV was significantly different from the effect of AVC-AVC (Fig. 5F), and a substantial level of percent synergy was also seen in the 3-D model (Fig. 5L).

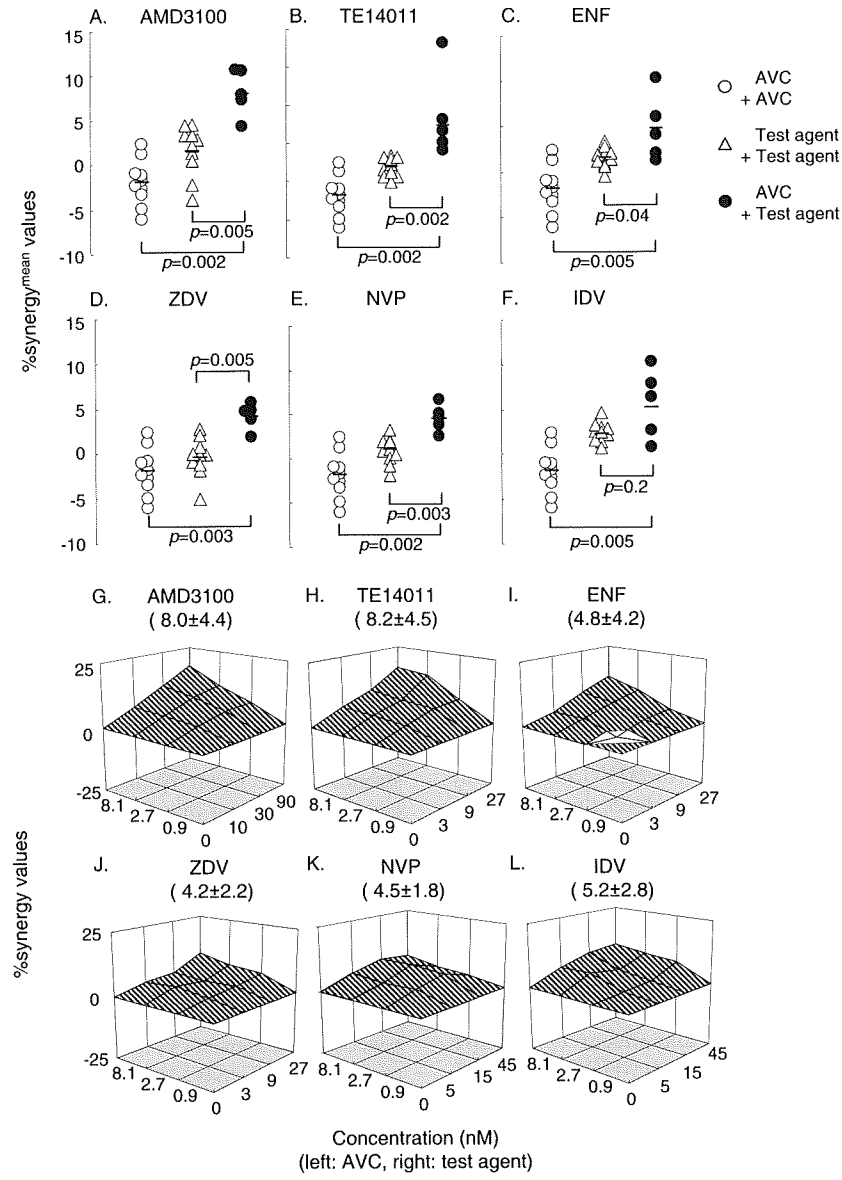

FIG. 5. Effects of AVC in combination with other anti-HIV-1 agents against a 50:50 mixture of R5-HIV-1_{Ba-L} and X4-HIV-$1_{ERS104pre}$. PHA-PBMCs were exposed to a 50:50 mixture of R5-HIV-1_{Ba-L} and X4-HIV-$1_{ERS104pre}$ and cultured in the presence of AVC in combination with AMD3100 (A), TE14011 (B), ENF (C), ZDV (D), NVP (E), or IDV (F) for 7 days, and the amounts of p24 Gag proteins in the culture supernatants were determined. Differences in the %synergy^{mean} values between AVC-AVC, test agent-test agent, and AVC-test agent were examined by using the Wilcoxon rank sum test. A statistically significant difference, or a strong trend, was observed for all combinations except between IDV-IDV and AVC-IDV ($P = 0.2$). The short bars indicate the arithmetic means obtained. The average percent synergy values for the AVC-test agent combinations were also plotted in 3-D graphs, as determined on the basis of the method of Prichard et al. (see the legend to Fig. 2) (G to L). Assays with AVC in combination with each drug and the same-drug combination were performed 5 times and 10 times, respectively. All assays were conducted in duplicate.

It was apparent that the %synergy^{mean} values of AVC-AMD3100 and AVC-TE14011 were greater than those of AVC plus any of the four antiviral agents (ENF, ZDV, NVP, and IDV). We therefore examined whether the apparent differences were statistically significant using the Wilcoxon rank sum test. The %synergy^{mean} values for AVC-AMD3100 were greater than those for AVC-ZDV ($P = 0.0472$) and AVC-NVP ($P = 0.0472$) but not those for AVC-ENF ($P = 0.1745$) and AVC-IDV ($P = 0.4647$). The %synergy^{mean} values of AVC-TE14011 were not statistically different from those of AVC plus any of the four agents ($P > 0.05$). Thus, even on the basis of a limited number of experiments, there were cases in which AVC-AMD3100 produced statistically greater synergism compared with the levels of synergism obtained with combinations of AVC and other conventional drugs. However, given the fact that the methodology used in the present study may as yet produce overestimates of synergy and the variability of the responses obtained by comparison of the combinations may also affect the analysis, it should be stressed that the effects of combinations of another CCR5 inhibitor(s) with another CXCR4 inhibitor(s) should be examined to confirm such synergism.

DISCUSSION

In the present study, we demonstrated that AVC exerts synergistic activity against HIV-$1_{Ba\text{-}L}$ in vitro when it is combined with ZDV, NVP, IDV, or ENF. These results are generally consistent with the data reported by Tremblay and colleagues, who examined two experimental CCR5 inhibitors, TAK220 and SCH-C, in combination with ZDV, lamivudine, IDV, efavirenz, or ENF for their effects against R5-HIV-1 isolates (38, 39).

Another CCR5 inhibitor, MVC, has recently received accelerated approval by the FDA for use in combination with other antiretroviral agents for the treatment of R5-HIV-1 in adults whose viral loads remain detectable despite existing antiviral treatment or who have multiple-drug-resistant viruses. In a recent 48-week data set from the MERIT study conducted with antiretroviral therapy-naïve subjects infected with R5-HIV-1 (32), 70.6% of the patients receiving MVC achieved HIV-1 RNA levels of less than 400 copies/ml, whereas 73.1% of the patients in the efavirenz group achieved HIV-1 RNA levels of less than 400 copies/ml, which met the criteria for noninferiority. However, when the HIV-1 RNA cutoff level of less than 50 copies/ml was used, noninferiority could not be confirmed. These data suggest that some of the patients who were determined to harbor R5-HIV-1 and who failed MVC therapy may have had X4-HIV-1, which MVC does not suppress.

It may be reasonable to suggest that R5-HIV-1 is not highly dominant in those infected with HIV-1. Indeed, the prevalence levels of R5- and X4-tropic viruses in patients with HIV-1 infection vary depending on the cohort examined. Demarest et al. demonstrated that the majority of drug-naïve and drug-experienced HIV-1-infected individuals harbored R5-HIV-1 (88% and 67%, respectively), while a mixture of R5- and X4-tropic viruses was seen in 12 and 28% of those individuals, respectively, and X4-tropic virus was seen in only 0 and 5% of those individuals, respectively (8). Fätkenheuer et al. have reported that the overall prevalence of R5-HIV-1 was 94% among the individuals whom they examined (11), while Daar et al. showed that 59.5% of 126 children and adolescents harbored R5-HIV-1 and the rest (40.5%) harbored viruses with dual or mixed tropisms (5). Taken together, the presence or absence of X4-HIV-1 in individuals who are to receive a CCR5 inhibitor, regardless of their positivity for X4-HIV-1, appears to be a critical factor for successful treatment with CCR5 inhibitor-containing regimens.

Using the Combo method (see below), we found that there were significant synergistic effects when AVC was combined with ZDV, NVP, IDV, or ENF and tested against HIV-$1_{Ba\text{-}L/104pre}$ (Fig. 5C to F). Interestingly, only a lower level of synergism was observed when AVC was combined with TAK779. When AVC was combined with SCH-C, no synergism was seen (Fig. 4A and C). In this regard, we have previously observed that the binding pockets for AVC, SCH-C, and TAK779 are all located in the same hydrophobic cavity within CCR5, although their binding profiles differ substantially from each other (17). We analyzed the interactions of these three inhibitors in relation to wild-type CCR5 ($CCR5_{WT}$). When $CCR5_{WT}$-overexpressed Chinese hamster ovarian cells were exposed to ^{3}H-labeled AVC, followed by the addition of unlabeled SCH-C, ^{3}H-labeled AVC binding to CCR5 was reduced only moderately. When the interaction between ^{3}H-labeled AVC and unlabeled TAK779 was examined, ^{3}H-labeled AVC binding to $CCR5_{WT}$ was not significantly replaced by unlabeled TAK779 binding. On the contrary, when ^{3}H-labeled SCH-C was added first and then unlabeled AVC was added, the binding of ^{3}H-labeled SCH-C to $CCR5_{WT}$ was significantly blocked, suggesting that AVC effectively replaced the ^{3}H-labeled SCH-C and bound to $CCR5_{WT}$. The binding of ^{3}H-labeled TAK779 was likewise blocked by the addition of unlabeled AVC, although the extent of replacement of ^{3}H-labeled TAK779 by AVC was less compared to the extent of replacement of ^{3}H-labeled SCH-C by AVC. These results appear to be explained at least in part by the binding of these three inhibitors to the same hydrophobic cavity within CCR5, although their binding profiles are different from each other and their affinities of binding to $CCR5_{WT}$ are also different (17). Whatever the mechanism, the present data suggest that the combination of small-molecule CCR5 inhibitors does not seem to bring about synergistic activity and that caution should perhaps be used when the use of combinations of multiple CCR5 inhibitors is considered.

Notably, the most potent synergism was seen when AVC was combined with AMD3100 or TE14011, as examined against HIV-$1_{Ba\text{-}L/104pre}$ (Fig. 5A and B). The synergy values for AVC-AMD3100 and AVC-TE14011 were greater (8.0 ± 4.4 and 8.2 ± 4.5, respectively) than those for any other combination (Fig. 5G and H). Hirsch's group has also examined the effects of the combination of aminooxypentane-RANTES and a derivative of stroma-derived factor 1β, using a mixture of R5- and X4-HIV-1 isolates, and found that these two agents effectively suppressed their replication, although they did not compare the effects of CCR5 inhibitors or CXCR4 inhibitors plus other FDA-approved anti-HIV-1 agents (31). The mechanism of the potent synergism with AVC plus each of the two CXCR4 inhibitors observed in the present study is not clear at this time. In this regard, Singer et al. have demonstrated that CCR5, CXCR4, and CD4 are apposed predominantly on cellular microvilli and apparently form homogeneous microclusters in all cell types examined, including macrophages and T cells (34). Such a spatial distribution of the surface cellular molecules involved in HIV-1's cellular entry may be related to the observed antiviral synergism, possibly through the concurrent CCR5 inhibitor and CXCR4 inhibitor binding to target molecules, which might result in synergistic steric hindrance or conformational changes in such surface molecules, leading to the inhibition of HIV-1's gp120/gp41 binding to and/or fusion with the target cells.

In the present study, in order to assess the effects of the combination of AVC with other drugs, we developed a system, designated the Combo method, which provides (i) a flexible choice of interaction models, (ii) the use of nonparametric statistical methods to obtain *P* values for comparisons, and (iii) flexibility with respect to the experimental design (e.g., checkerboard and constant-ratio designs). It is of note that when AVC was combined with itself, there was an indication of synergism, as assessed by CIs greater than CI at an inhibitory effect of 75%. This result was thought to represent a limitation or error inherent to the variability of the cell-based assay data obtained and/or the median-effect method used. Indeed, as has been noted by others (21), a "combination effect" is often defined on the basis of the empirical CI values (e.g., <0.9 for synergy and >1.1 for antagonism), irrespective of the interassay variability, and no adjustments for multiple comparisons

are generally made, producing an increased potential to overestimate the combination effects.

The variability of the cell-based assay data in determining the biological profiles of HIV-1, including its infectivity, replication competence, and cytopathic effect, stems from the very nature of the replication profiles of HIV-1 in culture. Unlike the bacterial multiplication profile, for which inhibition by antibiotics is arithmetically more predictable than is the case with HIV-1 replication, HIV-1 replication involves profuse but variable numbers of infectious progeny virions produced from a single infected cell. Indeed, the estimated number of progeny HIV-1 virions produced by a single HIV-1-exposed cell in our previous study ranged from 3.5×10^2 to 1.2×10^3 (14), while Layne et al. reported that such numbers ranged from 6×10^2 to 2.6×10^6 virions per cell (15). Moreover, the infectivity and replication competence of the HIV-1 inoculum can vary in the interassay as well as the intra-assay context. In fact, it is difficult to determine what portion of the virions used in a cell-based assay is infectious and replication competent. Layne et al. estimated the ratios of infectious to noninfectious virions using syncytium-forming units, which represents the infection of individual target cells by the number of cell-free virus counted (24) and which ranges from 4.1×10^{-4} to 3.6×10^{-7} (15). However, the number of virions produced in culture and their infectious potency also vary depending on the types of cells, particularly when target PHA-PBMCs are generated from different donors. Also, there should be variability in terms of the infectivity depending on the conditions of how and where the virus inoculum was generated and stored prior to the assay (16). In addition, if 100% viral infectivity suppression is not achieved in cell culture, a viral breakthrough tends to occur, since a continuous increase in the HIV-1 inoculum size occurs over the culture period and also contributes to the variability of the antiviral data. It is also true that the cell-based assays measure the cumulative effects of inhibitors over multiple cycles, which results in a substantial overestimation of synergy (12). It is noteworthy that the standard deviations of the EC_{50}s of the three CCR5 inhibitors (AVC, SCH-C, and TAK779) were relatively large (Table 1). In this regard, we have previously reported that much greater variability in the EC_{50}s for AVC compared to that for other classes of antiretroviral agents can be seen (18, 23). This variability most likely stems from that fact that the amounts of CCR5 receptors expressed on PBMCs differ substantially from one PBMC donor to another. Thus, evaluations of the antiviral effects of drug combinations require cautious interpretation of the data, including the use of statistical analyses to judge whether the differences between drug combinations are significant.

Using the Combo method described here, we compared the $\%synergy^{mean}$ values for AVC-AMD3100 with those for AVC-ENF, AVC-ZDV, AVC-NVP, and AVC-IDV (Fig. 5). Except in two instances, the effect of the combination of AVC with AMD3100 or TE14011 did not statistically exceed the effects of AVC plus other FDA-approved antiviral agents (Fig. 5) when the $\%synergy^{mean}$ values were examined. This observation that the synergism of AVC and a CXCR4 inhibitor failed to significantly exceed the effect of AVC in combination with the other antiviral agents tested could be due to the fact that the present study was not formally designed or powered for a direct comparison of the $\%synergy^{mean}$ values of AVC-AMD3100 and AVC-TE14011 against those of AVC plus FDA-approved antiretroviral drugs, with the result being that the number of experimental results evaluated for this comparison was quite small ($n = 5$). Larger experiments would likely be able to detect these differences as being significant. However, in our limited experiments, there was a tendency for the $\%synergy^{mean}$ values to be greater when AVC was combined with CXCR4 inhibitors than when AVC was combined with other compounds, even when this was not demonstrated statistically.

In the present study, cytotoxicity was virtually negligible at all concentrations and with all combinations examined. However, it is of note that although in the preclinical testing of AVC it was administered to monkeys at high doses over 9 months and no toxicity was observed, in phase IIb clinical trials, AVC caused grade 4 hepatotoxicity in 5 of 281 individuals receiving the drug and its development was abruptly terminated (25). Nevertheless, another CCR5 inhibitor, MVC, has been well tolerated, exerts significant antiviral effects, and has now been clinically used, suggesting that the hepatotoxicity of AVC is due to its chemical/structural properties and is not inherent to CCR5 inhibitors.

In conclusion, the present data demonstrate a tendency toward greater synergism when AVC is combined with either of the two CXCR4 inhibitors than when AVC is combined with other FDA-approved anti-HIV-1 agents, suggesting that the development of effective CXCR4 inhibitors may be important to increasing the efficacies of CCR5 inhibitors.

ACKNOWLEDGMENTS

This work was supported in part by the Intramural Research Program of the Center for Cancer Research, National Cancer Institute, National Institutes of Health, and in part by a Grant-in-Aid for Scientific Research (Priority Areas) from the Ministry of Education, Culture, Sports, Science, and Technology of Japan (Monbu-Kagakusho), a Grant for Promotion of AIDS Research from the Ministry of Health, Welfare, and Labor of Japan (Kosei-Rohdosho; grant H15-AIDS-001), and a Grant to the Cooperative Research Project on Clinical and Epidemiological Studies of Emerging and Reemerging Infectious Diseases (Renkei Jigyo, grant 78, Kumamoto University) of Monbu-Kagakusho.

REFERENCES

1. **Alkhatib, G., C. Combadiere, C. C. Broder, Y. Feng, P. E. Kennedy, P. M. Murphy, and E. A. Berger.** 1996. CC CKR5: a RANTES, MIP-1alpha, MIP-1beta receptor as a fusion cofactor for macrophage-tropic HIV-1. Science **272:**1955–1958.
2. **Baba, M., O. Nishimura, N. Kanzaki, M. Okamoto, H. Sawada, Y. Iizawa, M. Shiraishi, Y. Aramaki, K. Okonogi, Y. Ogawa, K. Meguro, and M. Fujino.** 1999. A small-molecule, nonpeptide CCR5 antagonist with highly potent and selective anti-HIV-1 activity. Proc. Natl. Acad. Sci. USA **96:**5698–5703.
3. **Chou, T. C., and P. Talalay.** 1981. Generalized equations for the analysis of inhibitions of Michaelis-Menten and higher-order kinetic systems with two or more mutually exclusive and nonexclusive inhibitors. Eur. J. Biochem. **115:**207–216.
4. **Chou, T. C., and P. Talalay.** 1984. Quantitative analysis of dose-effect relationships: the combined effects of multiple drugs or enzyme inhibitors. Adv. Enzyme Regul. **22:**27–55.
5. **Daar, E. S., K. L. Kesler, C. J. Petropoulos, W. Huang, M. Bates, A. E. Lail, E. P. Coakley, E. D. Gomperts, and S. M. Donfield.** 2007. Baseline HIV type 1 coreceptor tropism predicts disease progression. Clin. Infect. Dis. **45:**643–649.
6. **De Clercq, E.** 2002. Strategies in the design of antiviral drugs. Nat. Rev. Drug Discov. **1:**13–25.
7. **De Clercq, E., N. Yamamoto, R. Pauwels, J. Balzarini, M. Witvrouw, K. De Vreese, Z. Debyser, B. Rosenwirth, P. Peichl, R. Datema, et al.** 1994. Highly potent and selective inhibition of human immunodeficiency virus by the bicyclam derivative JM3100. Antimicrob. Agents Chemother. **38:**668–674.
8. **Demarest, J., T. Bonny, C. Vavro, C. Labranche, K. Kitrinos, C. Mcdanal, S. Sparks, S. Chavers, S. Castillo, D. Elrick, D. Mccarty, J. Whitcomb, W.**

Huang, C. Petropoulos, and S. Piscitell. 2004. HIV-1 co-receptor tropism in treatment naive and experienced subjects, abstr. H-1136. Abstr. 44th Intersci. Conf. Antimicrob. Agents Chemother. American Society for Microbiology, Washington, DC.

9. **Deng, H., R. Liu, W. Ellmeier, S. Choe, D. Unutmaz, M. Burkhart, P. Di Marzio, S. Marmon, R. E. Sutton, C. M. Hill, C. B. Davis, S. C. Peiper, T. J. Schall, D. R. Littman, and N. R. Landau.** 1996. Identification of a major co-receptor for primary isolates of HIV-1. Nature **381:**661–666.
10. **Dorr, P., M. Westby, S. Dobbs, P. Griffin, B. Irvine, M. Macartney, J. Mori, G. Rickett, C. Smith-Burchnell, C. Napier, R. Webster, D. Armour, D. Price, B. Stammen, A. Wood, and M. Perros.** 2005. Maraviroc (UK-427,857), a potent, orally bioavailable, and selective small-molecule inhibitor of chemokine receptor CCR5 with broad-spectrum anti-human immunodeficiency virus type 1 activity. Antimicrob. Agents Chemother. **49:**4721–4732.
11. **Fätkenheuer, G., A. L. Pozniak, M. A. Johnson, A. Plettenberg, S. Staszewski, A. I. Hoepelman, M. S. Saag, F. D. Goebel, J. K. Rockstroh, B. J. Dezube, T. M. Jenkins, C. Medhurst, J. F. Sullivan, C. Ridgway, S. Abel, I. T. James, M. Youle, and E. van der Ryst.** 2005. Efficacy of short-term monotherapy with maraviroc, a new CCR5 antagonist, in patients infected with HIV-1. Nat. Med. **11:**1170–1172.
12. **Ferguson, N. M., C. Fraser, and R. M. Anderson.** 2001. Viral dynamics and anti-viral pharmacodynamics: rethinking in vitro measures of drug potency. Trends Pharmacol. Sci. **22:**97–100.
13. **Gartner, S., P. Markovits, D. M. Markovitz, M. H. Kaplan, R. C. Gallo, and M. Popovic.** 1986. The role of mononuclear phagocytes in HTLV-III/LAV infection. Science **233:**215–219.
14. **Kageyama, S., D. T. Hoekzema, Y. Murakawa, E. Kojima, T. Shirasaka, D. J. Kempf, D. W. Norbeck, J. Erickson, and H. Mitsuya.** 1994. A C2 symmetry-based HIV protease inhibitor, A77003, irreversibly inhibits infectivity of HIV-1 in vitro. AIDS Res. Hum. Retrovir. **10:**735–743.
15. **Layne, S. P., M. J. Merges, M. Dembo, J. L. Spouge, S. R. Conley, J. P. Moore, J. L. Raina, H. Renz, H. R. Gelderblom, and P. L. Nara.** 1992. Factors underlying spontaneous inactivation and susceptibility to neutralization of human immunodeficiency virus. Virology **189:**695–714.
16. **Looney, D. J., S. Hayashi, M. Nicklas, R. R. Redfield, S. Broder, F. Wong-Staal, and H. Mitsuya.** 1990. Differences in the interaction of HIV-1 and HIV-2 with CD4. J. Acquir. Immune Defic. Syndr. **3:**649–657.
17. **Maeda, K., D. Das, H. Ogata-Aoki, H. Nakata, T. Miyakawa, Y. Tojo, R. Norman, Y. Takaoka, J. Ding, G. F. Arnold, E. Arnold, and H. Mitsuya.** 2006. Structural and molecular interactions of CCR5 inhibitors with CCR5. J. Biol. Chem. **281:**12688–12698.
18. **Maeda, K., H. Nakata, Y. Koh, T. Miyakawa, H. Ogata, Y. Takaoka, S. Shibayama, K. Sagawa, D. Fukushima, J. Moravek, Y. Koyanagi, and H. Mitsuya.** 2004. Spirodiketopiperazine-based CCR5 inhibitor which preserves CC-chemokine/CCR5 interactions and exerts potent activity against R5 human immunodeficiency virus type 1 in vitro. J. Virol. **78:**8654–8662.
19. **Maeda, K., K. Yoshimura, S. Shibayama, H. Habashita, H. Tada, K. Sagawa, T. Miyakawa, M. Aoki, D. Fukushima, and H. Mitsuya.** 2001. Novel low molecular weight spirodiketopiperazine derivatives potently inhibit R5 HIV-1 infection through their antagonistic effects on CCR5. J. Biol. Chem. **276:**35194–35200.
20. **Mosier, D. E., G. R. Picchio, R. J. Gulizia, R. Sabbe, P. Poignard, L. Picard, R. E. Offord, D. A. Thompson, and J. Wilken.** 1999. Highly potent RANTES analogues either prevent CCR5-using human immunodeficiency virus type 1 infection in vivo or rapidly select for CXCR4-using variants. J. Virol. **73:**3544–3550.
21. **Murga, J. D., M. Franti, D. C. Pevear, P. J. Maddon, and W. C. Olson.** 2006. Potent antiviral synergy between monoclonal antibody and small-molecule CCR5 inhibitors of human immunodeficiency virus type 1. Antimicrob. Agents Chemother. **50:**3289–3296.
22. **Nakata, H., M. Amano, Y. Koh, E. Kodama, G. Yang, C. M. Bailey, S. Kohgo, H. Hayakawa, M. Matsuoka, K. S. Anderson, Y. C. Cheng, and H. Mitsuya.** 2007. Activity against human immunodeficiency virus type 1, intracellular metabolism, and effects on human DNA polymerases of 4′-ethynyl-2-fluoro-2′-deoxyadenosine. Antimicrob. Agents Chemother. **51:**2701–2708.
23. **Nakata, H., K. Maeda, T. Miyakawa, S. Shibayama, M. Matsuo, Y. Takaoka, M. Ito, Y. Koyanagi, and H. Mitsuya.** 2005. Potent anti-R5 human immunodeficiency virus type 1 effects of a CCR5 antagonist, AK602/ONO4128/GW873140, in a novel human peripheral blood mononuclear cell nonobese diabetic-SCID, interleukin-2 receptor gamma-chain-knocked-out AIDS mouse model. J. Virol. **79:**2087–2096.
24. **Nara, P. L., and P. J. Fischinger.** 1988. Quantitative infectivity assay for HIV-1 and-2. Nature **332:**469–470.
25. **Nichols, W. G., H. M. Steel, T. Bonny, K. Adkison, L. Curtis, J. Millard, K. Kabeya, and N. Clumeck.** 2008. Hepatotoxicity observed in clinical trials of aplaviroc (GW873140). Antimicrob. Agents Chemother. **52:**858–865.
26. **Nishizawa, R., T. Nishiyama, K. Hisaichi, N. Matsunaga, C. Minamoto, H. Habashita, Y. Takaoka, M. Toda, S. Shibayama, H. Tada, K. Sagawa, D. Fukushima, K. Maeda, and H. Mitsuya.** 2007. Spirodiketopiperazine-based CCR5 antagonists: lead optimization from biologically active metabolite. Bioorg. Med. Chem. Lett. **17:**727–731.
27. **Prichard, M. N., L. E. Prichard, W. A. Baguley, M. R. Nassiri, and C. Shipman, Jr.** 1991. Three-dimensional analysis of the synergistic cytotoxicity of ganciclovir and zidovudine. Antimicrob. Agents Chemother. **35:**1060–1065.
28. **Prichard, M. N., L. E. Prichard, and C. Shipman, Jr.** 1993. Strategic design and three-dimensional analysis of antiviral drug combinations. Antimicrob. Agents Chemother. **37:**540–545.
29. **Prichard, M. N., and C. Shipman, Jr.** 1990. A three-dimensional model to analyze drug-drug interactions. Antivir. Res. **14:**181–205.
30. **Raport, C. J., J. Gosling, V. L. Schweickart, P. W. Gray, and I. F. Charo.** 1996. Molecular cloning and functional characterization of a novel human CC chemokine receptor (CCR5) for RANTES, MIP-1beta, and MIP-1alpha. J. Biol. Chem. **271:**17161–17166.
31. **Rusconi, S., S. La Seta Catamancio, P. Citterio, E. Bulgheroni, F. Croce, S. H. Herrmann, R. E. Offord, M. Galli, and M. S. Hirsch.** 2000. Combination of CCR5 and CXCR4 inhibitors in therapy of human immunodeficiency virus type 1 infection: in vitro studies of mixed virus infections. J. Virol. **74:**9328–9332.
32. **Saag, M., P. Ive, J. Heera, M. Tawadrous, E. DeJesus, N. Clumeck, D. Cooper, A. Horban, L. Mohapi, H. Mingrone, G. Reyes-Teran, S. Walmsley, F. Hackman, E. Ryst, and H. Mayer.** 2007. A multicenter, randomized, double-blind, comparative trial of a novel CCR5 antagonist, maraviroc versus efavirenz, both in combination with Combivir (zidovudine [ZDV]/lamivudine [3TC]), for the treatment of antiretroviral naive patients infected with R5 HIV 1: week 48 results of the MERIT study. 4th Int. AIDS Soc. Conf. HIV Pathogenesis, Treatment, Prevention, abstr. WESS104.
33. **Shirasaka, T., R. Yarchoan, M. C. O'Brien, R. N. Husson, B. D. Anderson, E. Kojima, T. Shimada, S. Broder, and H. Mitsuya.** 1993. Changes in drug sensitivity of human immunodeficiency virus type 1 during therapy with azidothymidine, dideoxycytidine, and dideoxyinosine: an in vitro comparative study. Proc. Natl. Acad. Sci. USA **90:**562–566.
34. **Singer, I. I., S. Scott, D. W. Kawka, J. Chin, B. L. Daugherty, J. A. DeMartino, J. DiSalvo, S. L. Gould, J. E. Lineberger, L. Malkowitz, M. D. Miller, L. Mitnaul, S. J. Siciliano, M. J. Staruch, H. R. Williams, H. J. Zweerink, and M. S. Springer.** 2001. CCR5, CXCR4, and CD4 are clustered and closely apposed on microvilli of human macrophages and T cells. J. Virol. **75:**3779–3790.
35. **Strizki, J. M., S. Xu, N. E. Wagner, L. Wojcik, J. Liu, Y. Hou, M. Endres, A. Palani, S. Shapiro, J. W. Clader, W. J. Greenlee, J. R. Tagat, S. McCombie, K. Cox, A. B. Fawzi, C. C. Chou, C. Pugliese-Sivo, L. Davies, M. E. Moreno, D. D. Ho, A. Trkola, C. A. Stoddart, J. P. Moore, G. R. Reyes, and B. M. Baroudy.** 2001. SCH-C (SCH 351125), an orally bioavailable, small molecule antagonist of the chemokine receptor CCR5, is a potent inhibitor of HIV-1 infection in vitro and in vivo. Proc. Natl. Acad. Sci. USA **98:**12718–12723.
36. **Tamamura, H., K. Hiramatsu, S. Kusano, S. Terakubo, N. Yamamoto, J. O. Trent, Z. Wang, S. C. Peiper, H. Nakashima, A. Otaka, and N. Fujii.** 2003. Synthesis of potent CXCR4 inhibitors possessing low cytotoxicity and improved biostability based on T140 derivatives. Org. Biomol. Chem. **1:**3656–3662.
37. **Tamamura, H., K. Hiramatsu, M. Mizumoto, S. Ueda, S. Kusano, S. Terakubo, M. Akamatsu, N. Yamamoto, J. O. Trent, Z. Wang, S. C. Peiper, H. Nakashima, A. Otaka, and N. Fujii.** 2003. Enhancement of the T140-based pharmacophores leads to the development of more potent and biostable CXCR4 antagonists. Org. Biomol. Chem. **1:**3663–3669.
38. **Tremblay, C. L., F. Giguel, Y. Guan, T. C. Chou, K. Takashima, and M. S. Hirsch.** 2005. TAK-220, a novel small-molecule CCR5 antagonist, has favorable anti-human immunodeficiency virus interactions with other antiretrovirals in vitro. Antimicrob. Agents Chemother. **49:**3483–3485.
39. **Tremblay, C. L., F. Giguel, C. Kollmann, Y. Guan, T. C. Chou, B. M. Baroudy, and M. S. Hirsch.** 2002. Anti-human immunodeficiency virus interactions of SCH-C (SCH 351125), a CCR5 antagonist, with other antiretroviral agents in vitro. Antimicrob. Agents Chemother. **46:**1336–1339.
40. **Trkola, A., T. Dragic, J. Arthos, J. M. Binley, W. C. Olson, G. P. Allaway, C. Cheng-Mayer, J. Robinson, P. J. Maddon, and J. P. Moore.** 1996. CD4-dependent, antibody-sensitive interactions between HIV-1 and its co-receptor CCR-5. Nature **384:**184–187.
41. **Westby, M., M. Lewis, J. Whitcomb, M. Youle, A. L. Pozniak, I. T. James, T. M. Jenkins, M. Perros, and E. van der Ryst.** 2006. Emergence of CXCR4-using human immunodeficiency virus type 1 (HIV-1) variants in a minority of HIV-1-infected patients following treatment with the CCR5 antagonist maraviroc is from a pretreatment CXCR4-using virus reservoir. J. Virol. **80:**4909–4920.
42. **Wu, L., N. P. Gerard, R. Wyatt, H. Choe, C. Parolin, N. Ruffing, A. Borsetti, A. A. Cardoso, E. Desjardin, W. Newman, C. Gerard, and J. Sodroski.** 1996. CD4-induced interaction of primary HIV-1 gp120 glycoproteins with the chemokine receptor CCR-5. Nature **384:**179–183.

ACCOUNTS
of chemical research

Design of HIV Protease Inhibitors Targeting Protein Backbone: An Effective Strategy for Combating Drug Resistance

ARUN K. GHOSH,*,† BRUNO D. CHAPSAL,† IRENE T. WEBER,‡ AND HIROAKI MITSUYA§,⊥

†Departments of Chemistry and Medicinal Chemistry, Purdue University, West Lafayette, Indiana 47907, ‡Department of Biology, Molecular Basis of Disease Program, Georgia State University, Atlanta, Georgia 30303, §Departments of Hematology and Infectious Diseases, Kumamoto University School of Medicine, Kumamoto 860-8556, Japan, and ⊥Experimental Retrovirology Section, HIV and AIDS Malignancy Branch, National Cancer Institute, Bethesda, Maryland 20892

RECEIVED ON MAY 18, 2007

CONSPECTUS

The discovery of human immunodeficiency virus (HIV) protease inhibitors (PIs) and their utilization in highly active antiretroviral therapy (HAART) have been a major turning point in the management of HIV/acquired immune-deficiency syndrome (AIDS). However, despite the successes in disease management and the decrease of HIV/AIDS-related mortality, several drawbacks continue to hamper first-generation protease inhibitor therapies. The rapid emergence of drug resistance has become the most urgent concern because it renders current treatments ineffective and therefore compels the scientific community to continue efforts in the design of inhibitors that can efficiently combat drug resistance.

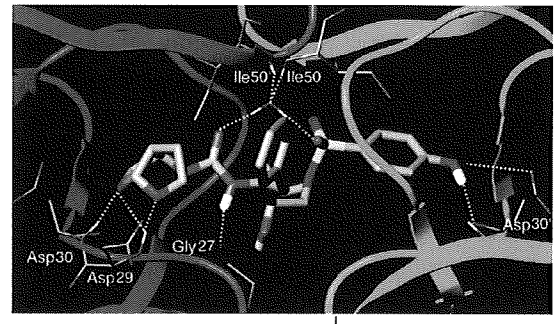

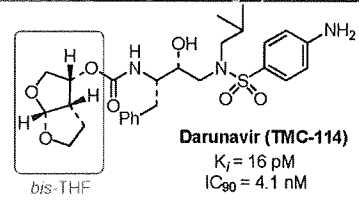

Darunavir (TMC-114)
K_i = 16 pM
IC_{90} = 4.1 nM

The present line of research focuses on the presumption that an inhibitor that can maximize interactions in the HIV-1 protease active site, particularly with the enzyme backbone atoms, will likely retain these interactions with mutant enzymes. Our structure-based design of HIV PIs specifically targeting the protein backbone has led to exceedingly potent inhibitors with superb resistance profiles.

We initially introduced new structural templates, particulary nonpeptidic conformationally constrained P_2 ligands that would efficiently mimic peptide binding in the S_2 subsite of the protease and provide enhanced bioavailability to the inhibitor. Cyclic ether derived ligands appeared as privileged structural features and allowed us to obtain a series of potent PIs. Following our structure-based design approach, we developed a high-affinity 3(*R*),3a(*R*),6a(*R*)-bis-tetrahydrofuranylurethane (bis-THF) ligand that maximizes hydrogen bonding and hyrophobic interactions in the protease S_2 subsite. Combination of this ligand with a range of different isosteres led to a series of exceedingly potent inhibitors.

Darunavir, initially TMC-114, which combines the bis-THF ligand with a sulfonamide isostere, directly resulted from this line of research. This inhibitor displayed unprecedented enzyme inhibitory potency (K_i = 16 pM) and antiviral activity (IC_{90} = 4.1 nM). Most importantly, it consistently retained is potency against highly drug-resistant HIV strains. Darunavir's IC_{50} remained in the low nanomolar range against highly mutated HIV strains that displayed resistance to most available PIs.

Our detailed crystal structure analyses of darunavir-bound protease complexes clearly demonstrated extensive hydrogen bonding between the inhibitor and the protease backbone. Most strikingly, these analyses provided ample evidence of the unique contribution of the bis-THF as a P_2-ligand. With numerous hydrogen bonds, bis-THF was shown to closely and tightly bind to the backbone atoms of the S_2 subsite of the protease. Such tight interactions were consistently observed with mutant proteases and might therefore account for the unusually high resistance profile of darunavir. Optimization attempts of the backbone binding in other subsites of the enzyme, through rational modifications of the isostere or tailor made P_2 ligands, led to equally impressive inhibitors with excellent resistance profiles.

The concept of targeting the protein backbone in current structure-based drug design may offer a reliable strategy for combating drug resistance.

Published on the Web 08/28/2007 www.pubs.acs.org/acr
10.1021/ar7001232 CCC: $40.75

Introduction

Acquired immunodeficiency syndrome (AIDS), a degenerative disease of the immune system, is caused by the human immunodeficiency virus (HIV).[1,2] The current statistics for global HIV/AIDS are staggering, as an estimated 40 million people worldwide are ailing with HIV/AIDS.[3] The discovery of HIV as the etiological agent for AIDS and subsequent investigation of the molecular events critical to the HIV replication cycle led to the identification of a number of important biochemical targets for AIDS chemotherapy.[4] During viral replication, *gag* and *gag-pol* gene products are translated into precursor polyproteins. These proteins are processed by the virally encoded protease to produce structural proteins and essential viral enzymes, including protease, reverse transcriptase, and integrase.[5] Therefore, inhibition of the virally encoded HIV protease was recognized as a viable therapeutic target.[6] Since the FDA approval of the first protease inhibitor (PI) in 1995,[7] several other PIs quickly followed. The development of these PIs and their introduction into highly active antiretroviral therapy (HAART) with reverse transcriptase inhibitors marked the beginning of an important era of AIDS chemotherapy. The HAART treatment regimens arrested the progression of AIDS and significantly reduced AIDS-related deaths in the United States and other industrialized nations.[8] Despite this undeniable success, there are severe limitations of the current treatment regimens including (i) debilitating side effects and drug toxicities, (ii) higher therapeutic doses due to "peptide-like" character, and (iii) expensive synthesis and high treatment cost. Perhaps most concerning of all is the emergence of drug resistance which renders treatment ineffective in a short time. The current HAART treatment regimens are not sufficiently potent to combat multidrug-resistant HIV strains. At least 40–50% of those patients who initially achieve favorable viral suppression to undetectable levels eventually experience treatment failure.[9] Additionally, 20–40% of antiviral therapy-naive individuals infected with HIV-1 have persistent viral replication under HAART, possibly due to primary transmission of drug-resistant HIV-1 variants.[10] The development of new PIs that address this issue is essential to the future management of HIV/AIDS.

Molecular Insight and Design Strategies To Combat Drug Resistance

Our structural analysis and comparison of protein–ligand X-ray structures of wild-type and mutant HIV proteases have revealed that the active site backbone conformation of mutant proteases is only minimally distorted.[11,12] This molecular insight led us to presume that an inhibitor which makes maximum interactions in the active site of HIV protease, particularly extensive hydrogen-bonding interactions in the protein backbone of the wild-type enzyme, will also retain these key interactions in the active site of mutant proteases. Our structure-based design to combat drug resistance is guided by the premise that an inhibitor exhibiting extensive hydrogen-bonding interactions with the protein backbone of the wild-type enzyme will likely retain potency against the mutant strains, since the mutations cannot easily eliminate the backbone interactions. Our objective is then focused on designing inhibitors that specifically target and maximize these interactions with backbone atoms. Another critical issue of current HAART therapies is the poor bioavailability of the current PIs. This in turn is responsible for much of the high-dose-related severe side effects and poor compliance issues.[13] Thus, our design of ligands and templates is also focused on designing non-peptidic cyclic/heterocyclic structures with improved bioavailability. Of particular interest, we plan to design cyclic ether or polyether-derived templates as these features are common to biologically active natural products. Such polyether templates may help improving aqueous solubility and increase oral bioavailability of PIs.

Development of Bis-THF as a High-Affinity P_2 Ligand

In a preliminary investigation based upon the X-ray structure of saquinavir-bound HIV-1 protease,[14] we designed a conformationally constrained cyclic ether-derived ligand to mimic the asparagine carbonyl binding in the S_2 subsite. As shown in Figure 1, inhibitor **1** with a 3(*S*)-tetrahydrofuranylurethane displayed an enzyme IC_{50} of 132 nM. The corresponding 3(*R*)-tetrahydrofuranyl derivative was significantly less potent (enzyme IC_{50} of 694 nM).[15,16] The potency-enhancing effect of 3(*S*)-tetrahydrofuran was further demonstrated in inhibitor **2** with a hydroxylethylene isostere.[16] Subsequently, this 3(*S*)-tetrahydrofuran was incorporated in an (*R*)-(hydroxyethyl)sulfonamide isostere to provide **3** (VX-476). This low-molecular-weight protease inhibitor was later approved by the FDA as amprenavir for the treatment of AIDS.[17]

A preliminary protein–ligand X-ray crystal structure of **1**-bound HIV-1 protease indicated that the oxygen atom of the tetrahydrofuran ring may be involved in a weak interaction with the backbone NHs of Asp 29 and Asp 30.[18] In an effort to further improve the potency of inhibitor **1**, we speculated that a fused bicyclic tetrahydrofuran (bis-THF) could effectively interact with both Asp 29 and Asp 30

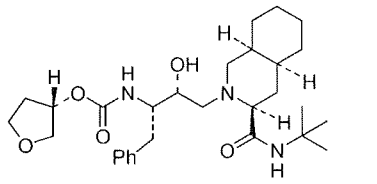

1 IC_{50} = 132 nM
CIC_{95} = 800 nM

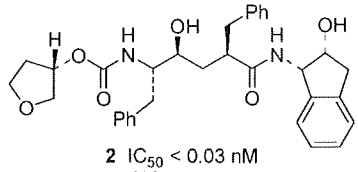

2 IC_{50} < 0.03 nM
CIC_{95} = 3 nM

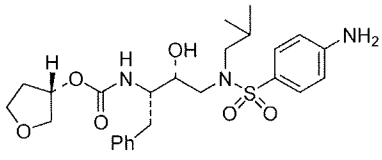

3 Ki = 0.6 nM
IC_{90} = 40 nM

FIGURE 1. Cyclic ether-containing protease inhibitors.

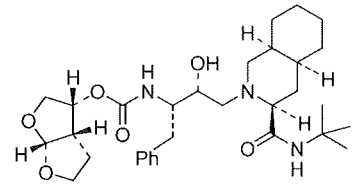

4 IC_{50} = 1.8 nM
CIC_{95} = 46 nM

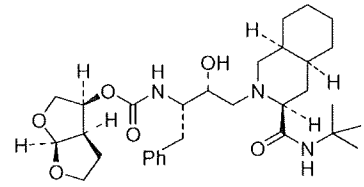

5 IC_{50} = 6.4 nM
CIC_{95} = 200 nM

FIGURE 2. Bis-THF-containing protease inhibitors.

amide NHs. Furthermore, the bicyclic rings of the bis-THF should offset loss of the P_3-hydrophobic quinoline ring of saquinavir. Interestingly, the bis-THF template is a subunit of ginkgolides A–C, an important class of natural products with significant biological activities.[19] Chemistry and biology of ginkgolides provided strong motivation for designing ginkgolide-derived ligands for the HIV protease substrate binding site.[19–21] Indeed, inhibitor **4** with a (3*R*,3a*S*,6a*R*)-bis-THF urethane showed a significant improvement in potency compared to **1** and its corresponding (*R*)-derivative (**5**).[15] Inhibitor **4** exhibited excellent enzyme inhibitory and antiviral potency (Figure 2).

Incorporation of the bis-THF ligand improved aqueous solubility and reduced molecular weight. Our systematic structure–activity relationship studies also ascertained that the stereochemistry (see inhibitor **5**, Figure 2), position of both oxygens (see inhibitors **6** and **7**, Figure 3), and ring sizes were critical to the activity of the inhibitor. An X-ray structure of **4**-bound HIV-1 protease revealed that both oxygens of the bis-THF ligand are within hydrogen-bonding distance to the Asp 29 and Asp 30 amide NHs in the S_2 subsite.[15]

Synthesis of the Bis-THF Ligand

The multistep synthesis of the optically active bis-THF ligand starting from (*R*)-malic acid was ineffective for the preparation of structural variants. We thus developed a three-step synthesis of racemic bis-THF followed by an immobilized lipase-catalyzed enzymatic resolution to provide optically active (3*R*,3a*S*,6a*R*)-3-hydroxyhexahydrofuro[2,3-*b*]furan (**12**) in high enantiomeric excess (>96% ee), as shown in Scheme 1. This synthesis helped us to extend the scope and utility of this privileged polyether-like non-peptidic ligand.[22] We recently reported two optically active syntheses of this ligand (Scheme 2). The first synthesis involved a novel stereoselective photochemical 1,3-dioxolane addition to 5(*S*)-benzyloxymethyl-2(5*H*)-furanone as the key step. The corresponding furanone was prepared in high enantiomeric excess by a lipase-catalyzed selective acylation of **15** followed by ring-closing olefin metathesis.[23] The second synthesis utilizes an ester-derived Ti–enolate-based highly stereoselective *anti*-aldol reaction as the key step.[24]

Development of Darunavir

We investigated the potency-enhancing effect of the bis-THF ligand with other isosteres. Incorporation of bis-THF in (*R*)-hydroxyethyl(sulfonamide) isosteres led to several exceedingly potent PIs with marked antiviral potency and drug-resistance profiles, as shown in Figure 4.[25]

Inhibitor **17** with a *p*-methoxysulfonamide as the P_2' ligand exhibited very impressive enzyme potency and antiviral activity. This PI has shown an excellent drug-resistance profile and good pharmacokinetic properties in laboratory animals.[26,27] It was later renamed TMC-126. In fact, inhibitor **17** showed >10-fold higher potency than the five currently available PIs (i.e., ritonavir (RTV), indinavir (IDV), saquinavir (SQV), nelfinavir (NFV), and amprenavir (APV)) in drug-sensitivity assays. It's IC_{50}s consistently remained as low as 0.3 nM.[26,27] Inhibitor **17** also displayed an unprecedented broad-spectrum activity against a large panel of primary, multidrug-resistant HIV-1 strains.[27]

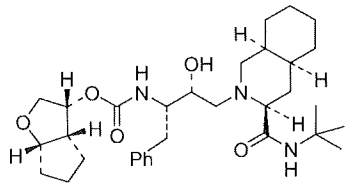

6 IC_{50} = 190 nM

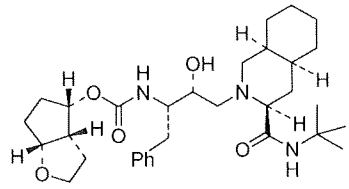

7 IC_{50} = 17 nM

FIGURE 3. Structure of inhibitors **6** and **7**.

SCHEME 1. Efficient Optically Active Synthesis of Bis-THF Ligand

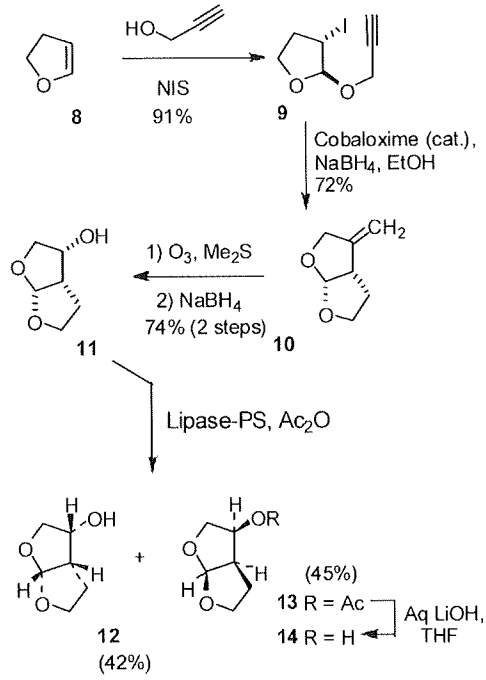

Incorporation of bis-THF into a *p*-aminosulfonamide isostere led to inhibitor **18**. Inhibitor **18** also showed unprecedented antiviral activity and outperformed most of the other currently available PIs against HIV-1_{Ba-L} by a 6–13-fold difference in IC_{50} values (Table 1).[28] Furthermore, this PI suppressed the replication of HIV-2 isolates with the most potent activity. It was later renamed TMC-114 or darunavir. When tested against HIV-1 strains that were selected for resistance to SQV, APV, IDV, NFV, or RTV after exposure to the various PIs at different concentrations (up to 5 μM), inhibitor **18** consistently and effectively suppressed viral infectivity and replication (IC_{50} values 0.003–0.029 μM) (Table 2), although lower activity was observed with APV-resistant strains (IC_{50} = 0.22 μM). In addition, inhibitor **18** potently blocked the replication of seven multidrug-resistant HIV-strains, isolated from heavily drug experienced patients with 9–14 mutations evidenced in their protease-encoding region.[28] Subsequent studies using a large panel of HIV-1 mutant strains provided further evidence of the remarkable profile of this inhibitor.[29]

SCHEME 2. Stereoselective Syntheses of the Bis-THF Ligand

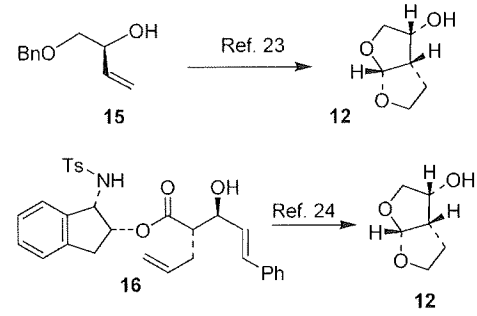

X-ray Crystal Structure of Darunavir and Evidence of Backbone Binding

High-resolution (1.10–1.34 Å) X-ray crystal structures of inhibitor **18** complexed with either wild-type HIV-1 protease or with two mutant proteases consistently showed strong hydrogen bonding of the bis-THF oxygens with the two Asp 29 and Asp 30 backbone amides (Figure 5).[28,30] New polar interactions with the Asp 30 side-chain carboxylate were also observed.[30] Additional hydrogen bonds were observed between the aniline moiety and the carbonyl oxygen and side-chain carboxylate of Asp 30′. Subsequent crystal structures of **18**-bound mutant proteases, including inhibitor **18**-bound resistant protease, clearly displayed a similar hydrogen-bonding pattern around the bis-THF ligand. These interactions seem to be crucial for maintaining the high affinity of the inhibitor

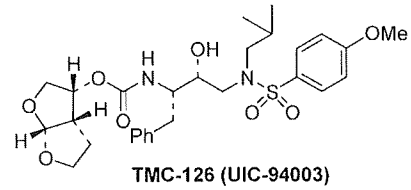

TMC-126 (UIC-94003)

17 K_i = 14 pM
IC_{90} = 1.4 nM

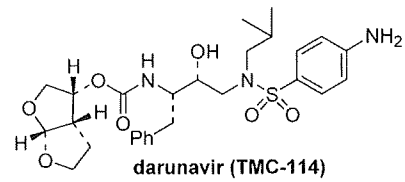

darunavir (TMC-114)

18 K_i = 16 pM
IC_{90} = 4.1 nM

FIGURE 4. Bis-THF-Derived Protease Inhibitors.

TABLE 1. Sensitivities of Selected Anti-HIV Agents against HIV-$1_{Ba\text{-}L}$, HIV-2_{ROD}, and HIV-2_{EHO}

		PIs, mean IC_{50} (nM) ± SDs[a]						
virus	cell type	AZT	SQV	APV	IDV	NFV	RTV	18 (TMC-114)
HIV-$1_{Ba\text{-}L}$[b]	PBMC	9 ± 1	18 ± 10	26 ± 5	25 ± 12	17 ± 4	39 ± 20	3 ± 0.3
HIV-2_{ROD}[c]	MT-2	18 ± 2	3 ± 0.2	230 ± 10	14 ± 6	19 ± 3	130 ± 60	3 ± 0.1
HIV-2_{EHO}[c]	MT-2	11 ± 2	6 ± 2	170 ± 50	11 ± 2	29 ± 18	240 ± 6	6 ± 3

[a] All assays were conducted in duplicate or triplicate; the data represent IC_{50} mean values (±SD) derived from the result of three independent experiments. [b] IC_{50} were evaluated with PHA–PBMC and the inhibition of p24 Gag protein production by the drug as an end point. [c] MT-2 cells were exposed to the virus and cultured, and IC_{50} values were determined by MTT assay.

TABLE 2. Activity of 18 against Laboratory PI-Resistant HIV-1

		IC_{50} (μM)[b]					
virus	amino acid substitution[a]	SQV	APV	IDV	NFV	RTV	18 (TMC-114)
HIV-1_{NL4-3}	wild type	0.009 (1)	0.027 (1)	0.011 (1)	0.020 (1)	0.018 (1)	0.003 ± 0.0005 (1)
HIV-$1_{SQV5\mu M}$	L10I, G48V, I54V, L90M	>1 (>111)	0.17 (6)	>1 (>91)	0.30 (15)	>1 (>56)	0.005 ± 0.0009 (2)
HIV-$1_{APV5\mu M}$	L10F, V32I, M46I, I54M, A71V, I84V	0.020 (2)	>1 (>37)	0.31 (28)	0.21 (11)	>1 (>56)	0.22 ± 0.05 (73)
HIV-$1_{IDV5\mu M}$	L10F, L24I, M46I, L63P, A71V, G73S, V82T	0.015 (2)	0.33 (12)	>1 (>91)	0.74 (37)	>1 (>56)	0.029 ± 0.0007 (10)
HIV-$1_{NFV5\mu M}$	L10F, D30N, K45I, A71V, T74S	0.031 (3)	0.093 (3)	0.28 (25)	>1 (>50)	0.09 (5)	0.003 ± 0.0002 (1)
HIV-$1_{RTV5\mu M}$	M46I, V82F, I84V	0.013 (1)	0.61 (23)	0.31 (28)	0.24 (12)	>1 (>56)	0.025 ± 0.006 (8)

[a] In PR. [b] MT-4 cells (10^4) were exposed to each HIV-1 (100x$TCID_{50}$s), and the inhibition of p24 Gag protein production by the drug was used as an end point. Numbers in parentheses represent the fold changes of IC_{50}s for each isolate relative to that of HIV-1_{NL4-3}.

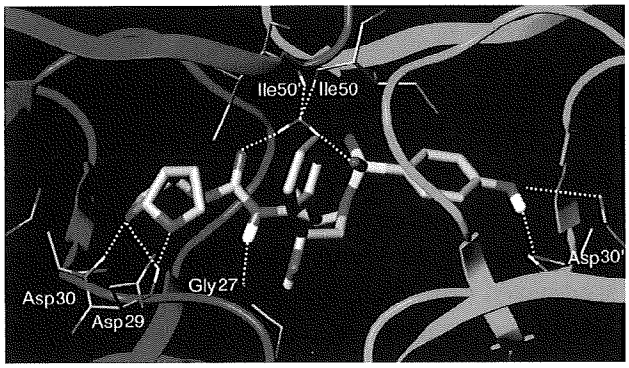

FIGURE 5. Interactions in X-ray crystal structure of **18**-bound HIV protease.

for the protease and appear to provide an explanation for the high potency against mutant proteases.[31–33]

Clinical Development of Darunavir

Inhibitor **18**, later renamed darunavir, showed a favorable pharmacokinetic profile in laboratory animals and was subsequently selected for further clinical studies. Tibotec (Belgium) carried out clinical developments of darunavir (**18**).[34] Darunavir (DRV) showed superior pharmacokinetic properties when coadministered with low doses of ritonavir.[35] Two-phase IIB clinical trials, POWER 1 and 2, are currently being performed on treatment-experienced patients to assess the safety, tolerability, and efficacy of darunavir with low doses of ritonavir (DRV/r) for 144 weeks. Early results at 24 weeks for one trial (POWER 1) showed that 77% of the DRV/r group vs. 25% for the control PI group achieved a ≥1 log_{10} viral load reduction, 53% under DRV/r vs. 18% reached a <50 cop-

TABLE 3. Sensitivity of HIV-1_{LAI} and HIV-$1_{Ba\text{-}L}$ against New PIs

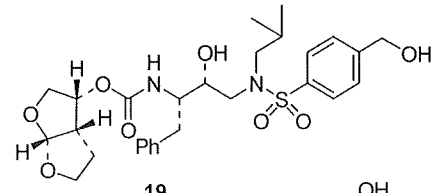

19

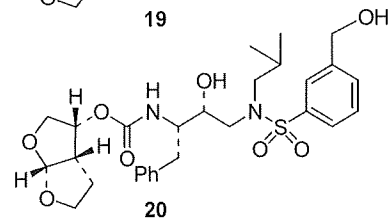

20

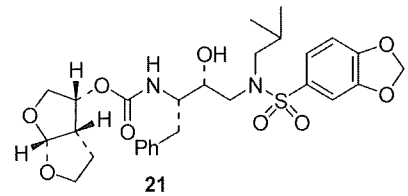

21

			IC_{50} (nm)		
virus	cell type	assay	**19**	**20**	**21**
HIV-1_{LAI}[a]	MT-2	MTT	5.3	28	0.22
HIV-1_{LAI}[b]	PBMC	p24	2.7	8	0.22
HIV-$1_{Ba\text{-}L}$[b]	PBMC	p24	3	9.3	0.33

[a] MT2 cells (2×10^3) were exposed to 100$TCID_{50}$ of HIV-1_{LAI} culture at various concentrations of PIs. [b] The IC_{50} values were determined by exposing the PHA-stimulated PBMC to the HIV-1 strain (50$TCID_{50}$ dose per 1×10^6 PBMC) at various concentrations of PI.

TABLE 4. Activity and Cross-Resistance Profile of Inhibitor 21

virus[a]	EC_{50} (nM)					
	SQV	RTV	NFV	APV	DRV	21 (GRL-98065)
HIV-$1_{ERS104pre}$ (wild-type X_4)	8 ± 3	25 ± 5	15 ± 4	29 ± 5	3.8 ± 0.7	0.5 ± 0.2
HIV-$1_{MDR/TM\ (X4)}$	180 ± 50 (23)	>1000 (>40)	>1000 (>67)	300 ± 40 (10)	4.3 ± 0.7 (1)	3.2 ± 0.6 (6)
HIV-$1_{MDR/MM\ (R5)}$	140 ± 40 (18)	>1000 (>40)	>1000 (>67)	480 ± 90 (17)	16 ± 7 (4)	3.8 ± 0.6 (8)
HIV-$1_{MDR/JSL\ (R5)}$	290 ± 50 (36)	>1000 (>40)	>1000 (>67)	430 ± 50 (15)	27 ± 9 (7)	6 ± 2 (12)
HIV-$1_{MDR/B\ (X4)}$	270 ± 60 (34)	>1000 (>40)	>1000 (>67)	360 ± 90 (12)	40 ± 10 (11)	3.9 ± 0.5 (8)
HIV-$1_{MDR/C\ (X4)}$	35 ± 4 (4)	>1000 (>40)	420 ± 60 (28)	250 ± 50 (9)	9 ± 5 (2)	2.7 ± 0.3 (5)
HIV-$1_{MDR/G\ (X4)}$	33 ± 5 (4)	>1000 (>40)	370 ± 50 (25)	320 ± 20 (11)	7 ± 5 (2)	3.4 ± 0.3 (7)

[a] The amino acid substitutions identified in the protease-encoding region compared to the consensus type B sequence cited from the Los Alamos database include L63P in HIV-1ERS104pre; L10I, K14R, R41K, M46L, I54V,L63P, A71V, V82A, L90M, I93L in HIV-1MDR/TM; L10I, K43T, M46L, I54V, L63P, A71V, V82A, L90M, and Q92K in HIV-1 MDR/MM; L10I, L24I, I33F, E35D, M36I, N37S, M46L, I54V, R57K, I62V, L63P, A71V, G73S, and V82A in HIV-1 MDR/JSL; L10I, K14R, L33I, M36I, M46I, F53I, K55R, I62V, L63P, A71V, G73S, V82A, L90M, and I93L in HIV-1 MDR/B; L10I, I15V, K20R, L24I, M36I, M46L, I54V, I62V, L63P, K70Q, V82A, and L89 M in HIV-1 MDR/C; and L10I, V11I, T12E, I15V, L19I, R41K, M46L, L63P, A71T, V82A, and L90 M in HIV-1 MDR/G. HIV-1ERS104 preserved as a source of wild-type HIV-1.

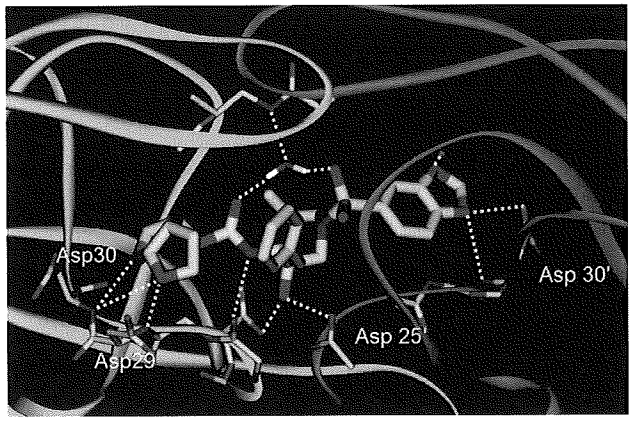

FIGURE 6. Crystal structure of inhibitor **21**-bound HIV-1 protease.

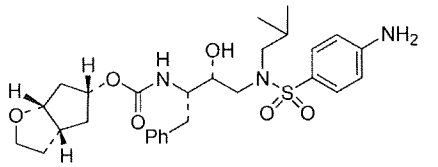

22 K_i = 0.14±0.02 nM
IC_{90} = 8 nM

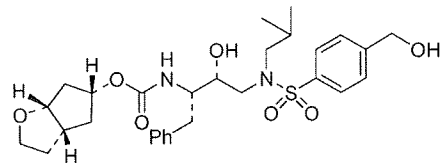

23 K_i = 0.0045±0.001 nM
IC_{90} = 1.8 nM

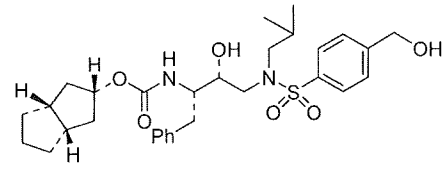

24 K_i = 5.3±0.3 nM
IC_{90} >1000 nM

FIGURE 7. Structures of Inhibitors **22–24**.

ies/mL viral load, CD_4+ cell count increased from baseline by 124 cells/mL in the DRV/r arm vs. 20 cells in the others.[36] A recent report at week 48 for the two trials showed that 61%

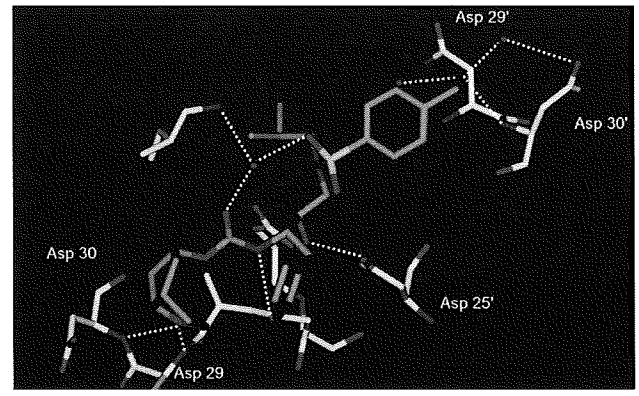

FIGURE 8. Inhibitor **23**-bound X-ray structure of HIV-1 protease.

of patients under DRV/r (600mg/100mg twice daily) maintained a >1 log_{10} reduction of viral load vs. baseline compared to 15% with the control PI arms.[37] Most impressively, 45% presented <50 viral copies/mL as opposed to 10% for the control arm. Darunavir was approved by the FDA in June 2006, as the first treatment for drug-resistant HIV.[38]

Bis-THF-Derived Novel PIs

We have further explored a number of P_2' sulfonamide functionalities to interact with the backbone atoms in the S_2' subsite. As shown in Table 3, inhibitors **19–21** displayed exceedingly potent inhibitory properties. Inhibitor **21**, which contains a benzodioxolanesulfonamide derivative as its P_2' ligand, provided impressive enzyme inhibitory (<5 pM) and antiviral potency.[39] The antiviral activity of the inhibitors was evaluated against wild-type clinical isolates HIV-1_{LAI} and HIV-1_{Ba-L} in PBMC cells and HIV-1_{LAI}-exposed MT-2 cells. Results of drug sensitivities are summarized in Table 3. Inhibitor **21**(GRL-98065) was then evaluated against both wild-type and HIV-1 mutant strains.[39] As shown in Table 4, inhibitor **21** outperformed most of the currently available PIs against multidrug-resistant HIV-1 clinical isolates, including DRV by a 2 to 10-fold improvement of activity.[39] Additional studies on

TABLE 5. Activity of 23 against a Wide Spectrum of HIV-1 Mutant Isolates

		IC_{50} (nM) values						
virus	mutations[a]	SQV	RTV	IDV	NFV	APV	DRV	**23**
1 (ET)	L10I	17	15	30	32	23	nd	3
2 (B)	L10I, K14R, L33I, M36I, M46I, F53L, K55R, I62V, L63P, A71V, G73S, V82A, L90M, I93L	230	>1000	>1000	>1000	290	10.2	15
3 (C)	I10L, I15V, K20R, M36I, M46L, I54V, K55R, I62V, L63P, K70Q, V82A, L89M	100	>1000	500	310	300	3.5	5
4 (G)	L10I, V11I, T12E, I15V, L19I, R41K, M46L, L63P, A71T, V82A, L90M	59	>1000	500	170	310	3.7	20
5 (TM)	L10I, K14R, R41K, M46L, I54V, L63P, A71V, V82A, L90M, I93L	250	>1000	>1000	>1000	220	3.5	4
6 (EV)	L10V, K20R, L33F, M36I, M46I, I50V, I54V, D60E, L63P, A71V, V82A, L90M	>1000	>1000	>1000	>1000	>1000	n.d.	52
7 (ES)	L10I, M46L, K55R, I62V, L63P, I72L, G73C, V77I, I84V, L90M	>1000	>1000	>1000	>1000	>1000	n.d.	31
8 (K)	L10F, D30N, K45I, A71V, T74S	20	57	260	>1000	68	3	3

[a] Amino acids substitutions identified in the protease-encoding region of HIV-1_{ET} (ET), HIV-1_{B} (B), HIV-1_{C} (C), HIV-1_{G} (G), HIV-1_{TM} (TM), HIV-1_{EV} (EV), HIV-1_{ES} (ES), HIV-1_{K} (NFV_R) as compared to consensus B sequence cited from the Los Alamos database.

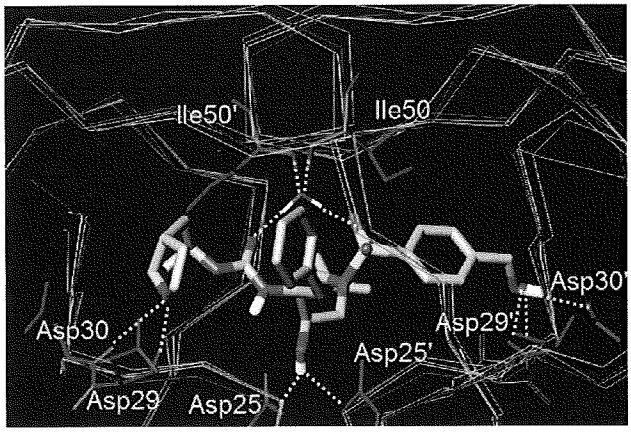

FIGURE 9. Inhibitor **23**-bound to the active site of wild-type HIV-1 protease superimposed upon the three most highly mutated drug-resistant proteases.

PI-resistant HIV-1 viral strains showed little sign of cross-resistance with inhibitor **21.**

As shown in Figure 6, the protein–ligand X-ray crystal structure of **21** revealed a pattern of four hydrogen-bonding interactions with the backbone residues of the protease similar to darunavir.[39] Because of its intriguing potency-enhancing effect and also its ability to maintain high potency against multidrug-resistant viral strains, the bis-THF ligand has been utilized for the development of other potent PIs. Most notably, researchers at GlaxoSmithKline explored an extremely potent inhibitor named brecanavir, which was a structural variant of inhibitor **21**.[40] The clinical development of this inhibitor was later abandoned reportedly due to difficulties in its formulation.

Design of Hexahydrocyclopentanofuranyl Ligand Based upon the "Backbone Binding" Concept

The remarkable ability of bis-THF-derived PIs to combat drug resistance has been documented through the clinical development of darunavir. Numerous protein–ligand X-ray crystal structures of bis-THF-containing PIs have now provided ample evidence of our concept that inhibitors with strong hydrogen-bonding interactions with the backbone atoms in the protease active site will be likely to maintain these interactions with mutant proteases and effectively combat drug resistance.[30–32] We next sought to design and develop PIs containing other novel ligands that could extensively interact with the backbone atoms. As outlined in Figure 7, we designed inhibitors **22** and **23** that contain a stereochemically defined bicyclic hexahydrocyclopentanofuran as a P_2 ligand.[41]

As shown, inhibitor **22**, with a 4-aminophenylsulfonamide as the P_2' ligand, exhibited very good enzyme inhibitory and antiviral activity. We then introduced a hydroxymethylphenylsulfonamide as a P_2' sulfonamide moiety with the intention of promoting hydrogen bonds between the hydroxyl oxygen and suitable backbone atoms in the S_2' subsite. Inhibitor **23** with a P_2' hydroxymethylphenylsulfonamide provided an impressive K_i value of 4.5 pM and antiviral IC_{50} of 1.8 nM. Compound **24** exhibited a >1100-fold loss of activity compared to that of inhibitor **23**, indicating the importance of the cyclopentanofuranyl oxygen's critical interactions in the active site. The X-ray crystal structure of **23**-bound HIV-1 protease (Figure 8) reveals that the P_2 ligand oxygen forms hydrogen bonding with the Asp 29 backbone NH.[41] The hydroxymethyl group of the P_2' sulfonamide moiety is within hydrogen-bonding distance to the Asp 30′ NH as well as the side-chain carboxylate (through a 10–20° rotation of the αC–βC bond of the residue).

Inhibitor **23** has shown very impressive antiviral activity against a panel of multidrug-resistant HIV-1 variants, and the results are shown in Table 5. It exerted high potency against six other variants with IC_{50} values ranging from 4 to 52 nM.[41] All the currently available protease inhibitors tested were

highly resistant to clinical strains. Overall, inhibitor **23** is highly active against a wide spectrum of drug-resistant variants and its activity is comparable to that of darunavir.

We have compared the X-ray structure of **23** with several reported protein–ligand X-ray structures of mutant proteases. A least-squares fit of the protease α-carbons atoms was performed, allowing comparison of the interactions of **23** with each of the mutant proteases. Figure 9 depicts the superimposition of the X-ray structure of **23** with the three most highly mutated drug-resistant proteases (PDB code and color: 2F81[41] with wild type, red; 2FDD,[42] blue; 1SGU,[43] green; 1HSH,[44] yellow). As can be seen, despite multiple mutations, there is only small change in active site backbone positions. Both the P_2 ligand oxygen and the P_2' hydroxymethyl group are within hydrogen-bonding distance to the respective backbone atoms and side-chain residues in the enzyme active site. On the basis of this analysis, it appeared that inhibitor **23** should retain good to excellent contacts with the backbone of mutant proteases.

Conclusion

The emergence of drug resistance to current antiretroviral treatment represents a major challenge that needs to be addressed with the development of a new generation of inhibitors with improved pharmacological profiles. Our structure-based design of new generation protease inhibitors incorporating novel cyclic-ether-derived ligands provided exceedingly potent inhibitors with impressive drug-resistance profiles. The inhibitors are designed to make extensive interactions, particularly hydrogen bonding, with the protein backbone of HIV-1 protease. Our extensive structural analysis of protein–ligand X-ray structures of bis-THF-containing inhibitors with wild-type and mutant proteases revealed retention of strong hydrogen-bonding interactions with the protein backbone. This structural element is only slightly distorted despite multiple amino acid mutations in the active site of HIV protease. One of our designed inhibitors, darunavir, has shown superior activity against multi-PI-resistant variants compared to other FDA-approved inhibitors. It has been recently approved as the first treatment of drug-resistant HIV. This important design concept targeting the active site protein backbone may serve as an effective strategy to combat drug resistance.

Financial support by the National Institutes of Health (GM 53386, AKG) is gratefully acknowledged. This work was also supported in part by the Intramural Research Program of the Center for Cancer Research, National Cancer Institute, National Institutes of Health, and in part by a Grant-in-aid for Scientific Research (Priority Areas) from the Ministry of Education, Culture, Sports, Science, and Technology of Japan (Monbu Kagakusho) and a Grant for Promotion of AIDS Research from the Ministry of Health, Welfare, and Labor of Japan. We also thank Dr. Geoff Bilcerand and Mr. Xiaoming Xu for helpful suggestions.

BIOGRAPHICAL INFORMATION

Arun K. Ghosh received his Ph.D. from the University of Pittsburgh and pursued postdoctoral research with Professor E. J. Corey at Harvard University. He was a Professor of Chemistry at the University of Illinois at Chicago from 1994 to 2005. From 2005 to present, he is a Professor in the departments of chemistry and medicinal chemistry at Purdue University.

Bruno D. Chapsal obtained his M.S. in chemistry from CPE Lyon, France, and received his Ph.D. from Stony Brook University, NY, under the direction of Professor Iwao Ojima. He is currently carrying out postdoctoral research in Professor Ghosh's laboratories.

Irene T. Weber received her Ph.D. from the University of Oxford, England, under the supervision of Professor Louise Johnson. She pursued postdoctoral research with Professor Thomas Steitz at Yale University. She was Professor of Microbiology and Immunology at Thomas Jefferson University in Philadelphia from 1991 to 2000. From 2001 to the present she is Professor of Biology and Chemistry at Georgia State University in Atlanta.

Hiroaki Mitsuya received his M.D. and Ph.D. from the Kumamoto University School of Medicine, Japan. He was a Visiting Scientist at the National Cancer Institute from 1982 to 1990. From 2001 to present, he is Principal Investigator & Chief, Experimental Retrovirology Section, HIV and AIDS Malignancy Branch, National Cancer Institute, Bethesda, MD. From 1997 to present, he is also Professor of Medicine and Chairman, Department of Internal Medicine, Kumamoto University School of Medicine, Japan.

FOOTNOTES

*To whom correspondence should be addressed. Fax: 765-496-1612. E-mail: akghosh@purdue.edu.

REFERENCES

1 Barre-Sinoussi, F.; Chermann, J. C.; Rey, F.; Nugeyre, M. T.; Chamaret, S.; Gruest, J.; Dauguet, C.; Axler-Blin, C.; Vezinet-Brun, F.; Rouzioux, C.; Rozenbaum, W.; Montagnier, L. Isolation of a T-lymphotropic Retrovirus from a Patient at Risk for Acquired Immune Deficiency Syndrome (AIDS). *Science* **1983**, *220*, 868–871.

2 Gallo, R. C.; Salahuddin, S. Z.; Popovic, M.; Shearer, G. M.; Kaplan, M.; Haynes, B. F.; Palker, T. J.; Redfield, R.; Oleske, J.; Safai, B.; White, G.; Foster, P.; Markham, P. D. Frequent Detection and Isolation of Cytopathic Retroviruses (HTLV-III) from Patients with AIDS and at Risk for AIDS. *Science* **1984**, *224*, 500–503.

3 The impact of AIDS on People and Societies/2006, report on the Global AIDS Epidemic, http://data.unaids.org/pub/GlobalReport/2006/2006_GR_CH04_en.pdf

4 De Clercq, E. New Approaches toward Anti-HIV Chemotherapy. *J. Med. Chem.* **2005**, *48*, 1297–1313.

5 Graves, M. C.; Lim, J. J.; Heimer, E. P.; Kramer, R. A. An 11-kDa Form of Human Immunodeficiency Virus Protease Expressed in Escherichia Coli is Sufficient for Enzymatic Activity. *Proc. Natl. Acad. Sci. U.S.A.* **1988**, *85*, 2449–2453.

6 Wlodawer, A.; Vondrasek, J. Inhibitors of HIV-1 Protease: A Major Success of Structure-Assisted Drug Design. *Annu. Rev. Biophys. Biomol. Struct.* **1998**, *27*, 249–284.

7 The First HIV Protease Inhibitors Approved by FDA. *Antiviral Agents Bull.* **1995**, *8*, 353–355.

8 Sepkowitz, K. A. AIDS—The First 20 Years. *N. Engl. J. Med.* **2001**, *344*, 1764–1772.

9 Grabar, S.; Pradier, C.; Le Corfec, E.; Lancar, R.; Allavena, C.; Bentata, M.; Berlureau, P.; Dupont, C.; Fabbro-Peray, P.; Poizot-Martin, I.; Costagliola, D. Factors Associated with Clinical and Virological Failure in Patients Receiving a Triple Therapy Including a Protease Inhibitor. *AIDS* **2000**, *14*, 141–149.

10 Wainberg, M. A.; Friedland, G. Public Health Implications of Antiretroviral Therapy and HIV Drug Resistance. *J. Am. Med. Assoc.* **1998**, *279*, 1977–1983.

11 Hong, L.; Zhang, X.; Hartsuck, J. A.; Tang, J. Crystal Structure of an In Vivo HIV-1 Protease Mutant in Complex with Saquinavir: Insights into the Mechanisms of Drug Resistance. *Protein Sci.* **2000**, *9*, 1898–1904.

12 Laco, G. S.; Schalk-Hihi, C.; Lubkowski, J.; Morris, G.; Zdanov, A.; Olson, A.; Elder, J. H.; Wlodawer, A.; Gustchina, A. Crystal Structures of the Inactive D30N Mutant of Feline Immunodeficiency Virus Protease Complexed with a Substrate and an Inhibitor. *Biochemistry* **1997**, *36*, 10696–10708.

13 Glesby, M. J. Toxicities and Adverse Effects of Protease Inhibitors. In *Protease Inhibitors in AIDS Therapy*; Ogden, R. C., Flexner, C. W., Eds.; Marcel Dekker: New York, 2001; pp 237–256.

14 Krohn, A.; Redshaw, S.; Ritchie, J. C.; Graves, B. J.; Hatada, M. H. Novel Binding Mode of Highly Potent HIV-Proteinase Inhibitors Incorporating the (R)-Hydroxyethylamine Isostere. *J. Med. Chem.* **1991**, *34*, 3340–3342.

15 Ghosh, A. K.; Kincaid, J. F.; Walters, D. E.; Chen, Y.; Chaudhuri, N. C.; Thompson, W. J.; Culberson, C.; Fitzgerald, P. M. D.; Lee, H. Y.; McKee, S. P.; Munson, P. M.; Duong, T. T.; Darke, P. L.; Zugay, J. A.; Schleif, W. A.; Axel, M. G.; Lin, J.; Huff, J. R. Nonpeptidal P_2 Ligands for HIV Protease Inhibitors: Structure-Based Design, Synthesis, and Biological Evaluation. *J. Med. Chem.* **1996**, *39*, 3278–3290.

16 Ghosh, A. K.; Thompson, W. J.; McKee, S. P.; Duong, T. T.; Lyle, T. A.; Chen, J. C.; Darke, P. L.; Zugay, J. A.; Emini, E. A.; Schleif, W. A.; Huff, J. R.; Anderson, P. S. 3-Tetrahydrofuran and Pyran Urethanes as High-Affinity P_2-Ligands for HIV-1 Protease Inhibitors. *J. Med. Chem.* **1993**, *36*, 292–294.

17 Kim, E. E.; Baker, C. T.; Dwyer, M. D.; Murcko, M. A.; Rao, B. G.; Tung, R. D.; Navia, M. A. Crystal Structure of HIV-1 Protease in Complex with VX-478, a Potent and Orally Bioavailable Inhibitor of the Enzyme. *J. Am. Chem. Soc.* **1995**, *117*, 1181–1182.

18 Ghosh, A. K.; Thompson, W. J.; Fitzgerald, P. M. D.; Culberson, J. C.; Axel, M. G.; McKee, S. P.; Huff, J. R.; Anderson, P. S. Structure-based Design of HIV-1 Protease Inhibitors: Replacement of two Amides and a 10π-Aromatic System by a Fused Bis-Tetrahydrofuran. *J. Med. Chem.* **1994**, *37*, 2506–2508.

19 Nakanishi, K. The Ginkgolides. *Pure Appl. Chem.* **1967**, *14*, 89–114.

20 Corey, E. J.; Kang, M. C.; Desai, M. C.; Ghosh, A. K.; Houpis, I. N. Total Synthesis of (+/−)-Ginkgolide-B. *J. Am. Chem. Soc.* **1988**, *110*, 649–651.

21 Corey, E. J.; Ghosh, A. K. Total Synthesis of Ginkgolide A. *Tetrahedron Lett.* **1988**, *29*, 3205–3206.

22 Ghosh, A. K.; Chen, Y. Synthesis and Optical Resolution of High Affinity P_2 Ligands for HIV-1 Protease Inhibitors. *Tetrahedron Lett.* **1995**, *36*, 505–508.

23 Ghosh, A. K.; Leschenko, S.; Noetzel, M. Stereoselective Photochemical 1,3-Dioxolane Addition to 5-Alkoxymethyl-2(5*H*)-furanone: Synthesis of Bis-Tetrahydrofuranyl Ligand for HIV Protease Inhibitor UIC-94017 (TMC-114). *J. Org. Chem.* **2004**, *69*, 7822–7829.

24 Ghosh, A. K.; Li, J.; Sridhar, P. R. A Stereoselective Anti-Aldol Route to (3*R*,3a*S*,6a*R*)-Hexahydrofuro[2,3-*b*]furan-3-ol: A Key Ligand for a New Generation of HIV Protease Inhibitors. *Synthesis* **2006**, *18*, 3015–3018.

25 Ghosh, A. K.; Kincaid, J. F.; Cho, W.; Walters, D. E.; Krishnan, K.; Hussain, K. A.; Koo, Y.; Cho, H.; Rudall, C.; Holland, L.; Buthod, J. Potent HIV Protease Inhibitors Incorporating High-Affinity P_2-Ligands and (*R*)-(Hydroxyethylamino)sulfonamide Isostere. *Bioorg. Med. Chem. Lett.* **1998**, *8*, 687–690.

26 Ghosh, A. K.; Pretzer, E.; Cho, H.; Hussain, K. A.; Duzgunes, N. Antiviral Activity of UIC-PI, a Novel Inhibitor of the Human Immunodeficiency Virus Type 1 Protease. *Antiviral Res.* **2002**, *54*, 29–36.

27 Yoshimura, K.; Kato, R.; Kavlick, M. F.; Nguyen, A.; Maroun, V.; Maeda, K.; Hussain, K. A.; Ghosh, A. K.; Gulnik, S. V.; Erickson, J. W.; Mitsuya, H. A Potent Human Immunodeficiency Virus Type 1 Protease Inhibitor, UIC-94003 (TMC-126), and Selection of a Novel (A28S) Mutation in the Protease Active Site. *J. Virol.* **2002**, *76*, 1349–1358.

28 Koh, Y.; Nakata, H.; Maeda, K.; Ogata, H.; Bilcer, G.; Devasamudram, T.; Kincaid, J. F.; Boross, P.; Wang, Y.-F.; Tie, Y.; Volarath, P.; Gaddis, L.; Harrison, R. W.; Weber, I. T.; Ghosh, A. K.; Mitsuya, H. Novel *bis*-Tetrahydrofuranylurethane-Containing Nonpeptidic Protease Inhibitor (PI) UIC-94017 (TMC114) with Potent Activity against Multi-PI-Resistant Human Immunodeficiency Virus In Vitro. *Antimicrob. Agents Chemother.* **2003**, *47*, 3123–3129.

29 De Meyer, S.; Azijn, H.; Surleraux, D.; Jochmans, D.; Tahri, A.; Pauwels, R.; Wigerinck, P.; de Bethune, M.-P. TMC114, a Novel Human Immunodeficiency Virus Type 1 Protease Inhibitor Active against Protease Inhibitor-Resistant Viruses, Including a Broad Range of Clinical Isolates. *Antimicrob. Agents Chemother.* **2005**, *49*, 2314–2321.

30 Tie, Y.; Boross, P. I.; Wang, Y.-F.; Gaddis, L.; Hussain, A. K.; Leshchenko, S.; Ghosh, A. K.; Louis, J. M.; Harrison, R. W.; Weber, I. T. High Resolution Crystal Structures of HIV-1 Protease with a Potent Non-Peptide Inhibitor (UIC-94017) Active against Multi-Drug-Resistant Clinical Strains. *J. Mol. Biol.* **2004**, *338*, 341–352.

31 Kovalevsky, A. Y.; Tie, Y.; Liu, F.; Boross, P. I.; Wang, Y.-F.; Leshchenko, S.; Ghosh, A. K.; Harrison, R. W.; Weber, I. T. Effectiveness of Nonpeptide Clinical Inhibitor TMC-114 on HIV-1 Protease with Highly Drug Resistant Mutations D30N, I50V, and L90M. *J. Med. Chem.* **2006**, *49*, 1379–1387.

32 Kovalevsky, A. Y.; Liu, F.; Leshchenko, S.; Ghosh, A. K.; Louis, J. M.; Harrison, R. W.; Weber, I. T. Ultra-High Resolution Crystal Structure of HIV-1 Protease Mutant Reveals Two Binding Sites for Clinical Inhibitor TMC114. *J. Mol. Biol.* **2006**, *363*, 161–173.

33 King, N. M.; Prabu-Jeyabalan, M.; Nalivaika, E. A.; Wigerinck, P.; de Bethune, M.-P.; Schiffer, C. A. Structural and Thermodynamic Basis for the Binding of TMC114 a Next-Generation Human Immunodeficiency Virus Type 1 Protease Inhibitor. *J. Virol.* **2004**, *78*, 12012–12021.

34 De Meyer, S.; Peters, M. Abstracts 533 and 620, 11th Conference on Retroviruses and Opportunistic Infections (CROI); Feb 8–11 2004, San Francisco, CA.

35 Hoetelmans, R.; van der Sandt, I.; De Pauw, M.; Struble, K.; Peeters, M.; van der Geest, R. TMC114, a Next Generation HIV Protease Inhibitor: Pharmacokinetics and Safety Following Oral Administration of Multiple Doses with or without Low Doses of Ritonavir in Healthy Volunteers; Abstract 549, 10th Conference on Retroviruses and Opportunistic Infections (CROI); Feb 2003, Boston, MA.

36 Katlama, C.; Carvalho, M. T. M.; Cooper, D.; De Backer, K.; Lefebvre, E.; Pedro, R.; Rombouts, K.; Stoehr, A.; Vangeneugden, T.; Woehrmann, A. TMC114/r Outperforms Investigators-selected PI(s) in 3-class-experienced Patients: Week 24 Efficacy Analysis of POWER 1 (TMC114-C213) [Poster WeOaIB0102], 3rd IAS Conference on HIV Pathogenesis and Treatment; July 24–27 2005, Rio de Janeiro, Brazil.

37 Clotet, B.; Bellos, N.; Molina, J.-M.; Cooper, D.; Goffard, J.-C.; Lazzarin, A.; Wohrmann, A.; Katlama, C.; Wilkin, T.; Haubrich, R.; Cohen, C.; Farthing, C.; Jayaweera, D.; Markowitz, M.; Ruane, P.; Spinosa-Guzman, S.; Lefebvre, E. Efficacy and Safety of Darunavir-Ritonavir at Week 48 in Treatment-experienced Patients with HIV-1 Infection in POWER 1 and 2: a Pooled Subgroup Analysis of Data from Two Randomised Trials. *Lancet* **2007**, *369*, 1169–1178.

38 FDA approves Darunavir on June 23, 2006: FDA approved new HIV treament for patients who do not respond to existing drugs. Please see http://www.fda.gov/bbs/topics/NEWS/2006/NEW01395.html

39 Amano, M.; Koh, Y.; Das, D.; Li, J.; Leschenko, S.; Wang, Y.-F.; Boross, P. I.; Weber, I. T.; Ghosh, A. K.; Mitsuya, H. A Novel *Bis*-Tetrahydrofuranylurethane-Containing Nonpeptidic Protease Inhibitor (PI), GRL-98065, Is Potent against Multi-PI-Resistant Human Immunodeficiency Virus *In Vitro*. *Antimicrob. Agents Chemother.* **2007**, *51*, 2143–2155.

40 Spaltenstein, A.; Kazmierski, W. M.; Miller, J. F.; Samano, V. Discovery of Next Generation Inhibitors of HIV Protease. *Curr. Top. Med. Chem.* **2005**, *5*, 1589–1607.

41 Ghosh, A. K.; Sridhar, P. R.; Leshchenko, S.; Hussain, A. K.; Li, J.; Kovalevsky, A. Y.; Walters, D. E.; Wedekind, J. E.; Grum-Tokars, V.; Das, D.; Koh, Y.; Maeda, K.; Gatanaga, H.; Weber, I. T.; Mitsuya, H. Structure-based Design of Novel HIV-1 Protease Inhibitors to Combat Drug Resistance. *J. Med. Chem.* **2006**, *49*, 5252–5261.

42 Miller, J. F.; Andrews, C. W.; Brieger, M.; Furfine, E. S.; Hale, M. R.; Hanlon, M. H.; Hazen, R. J.; Kaldor, I.; McLean, E. W.; Reynolds, D.; Sammond, D. M.; Spaltenstein, A.; Tung, R.; Turner, E. M.; Xu, R. X.; Sherrill, R. G. Ultra-Potent P_1 Modified Arylsulfonamide HIV Protease Inhibitors: The Discovery of GW0385. *Bioorg. Med. Chem. Lett.* **2006**, *16*, 1788–1794.

43 Clemente, J. C.; Moose, R. E.; Hemrajani, R.; Whitford, L. R.; Govindasamy, L.; Reutzel, R.; McKenna, R.; Agbandje-McKenna, M.; Goodenow, M. M.; Dunn, B. M. Comparing the Accumulation of Active- and Nonactive-site Mutations in the HIV-1 Protease. *Biochemistry* **2004**, *43*, 12141–12151.

44 Chen, Z.; Li, Y.; Chen, E.; Hall, D. L.; Darke, P. L.; Culberson, C.; Shafer, J. A.; Kuo, L. C. Crystal Structure at 1.9-Å Resolution of Human Immunodeficiency Virus (HIV) II Protease Complexed with L-735,524, an Orally Bioavailable Inhibitor of the HIV Proteases. *J. Biol. Chem.* **1994**, *269*, 26344–26348.

Hiroaki Mitsuya*,†, Kenji Maeda*, Debananda Das*, and Arun K. Ghosh‡

*The Experimental Retrovirology Section, HIV and AIDS Malignancy Branch, Center for Cancer Research, National Cancer Institute, Bethesda, Maryland 20892

†Department of Hematology and Infectious Diseases, Kumamoto University School of Medicine, Kumamoto 860–8556

‡Departments of Chemistry and Medicinal Chemistry, Purdue University, West Lafayette, Indiana 47907

Development of Protease Inhibitors and the Fight with Drug-Resistant HIV-1 Variants

I. Chapter Overview

The development of antiretroviral therapy for acquired immunodeficiency syndrome (AIDS) has witnessed one of the most dramatic progressions in the history of medicine. By the late 1980s, it had become apparent that combination chemotherapy with two nucleoside reverse transcriptase inhibitors (NRTIs) was more effective than NRTI monotherapy. However, only with the advent of protease inhibitors (PIs) in early 1990s, providing highly active antiretroviral therapy (HAART), significant clinical benefits became to be seen.

Advances in Pharmacology, Volume 56

1054-3589/08 $35.00
DOI: 10.1016/S1054-3589(07)56006-0